The Performance of Low-Rise Open Span Heavy Steel Structures In Extreme Winds

by

Joe R. Charlton, B.S., P.E.

A REPORT

IN

CIVIL ENGINEERING

Submitted to the Graduate Faculty
of Texas Tech University in
Partial Fulfillment of
the Requirements for
the Degree of

MASTER OF SCIENCE

IN

CIVIL ENGINEERING

TABLE OF CONTENTS

ABSTRACT

This report is an engineering study of the field performance of open span low-rise steel frame structures that have been subjected to extreme wind events such as hurricanes and tornadoes. The wind velocities in these events either approached or slightly exceeded the normal design values specified in ASCE 7-95. This report focuses specifically on the performance of heavy steel structures and does not include pre-engineered metal buildings. All types of building failures are observed and analyzed in this report, including roofing and secondary cladding component failures as well as main structural failures. In each case study, the probable cause of failure is determined and through an analysis of the different case studies, patterns of failure are identified. Through an analysis of the patterns of failure, recommendations for general design improvements are made and areas requiring further study are identified.

The study found that the main structural systems of heavy steel structures performed very well in these extreme winds. Virtually no damage was observed to any of the components of the main structural systems of the buildings, even when the wind velocities exceeded design values by as much as 30 percent. However, the components and cladding did not perform as well. In almost every instance of failure, at least some portion of the roof decking was removed. In most cases the damaged area was restricted to the windward edge of the roof/wall intersection. Another weak component was the overhead doors. In over half of the instances of damage, the overhead door was the first point of failure. The failure of the overhead door(s) then caused the failure of other building components.

LIST OF TABLES

LIST OF TABLES

LIST OF FIGURES

LIST OF FIGURES
(CONTINUED)

CHAPTER 1

INTRODUCTION

Each year in the United States wind storms, such as hurricanes and tornadoes, cause more economic losses than any other natural phenomenon (Simiu et al., 1996). Hurricanes are typically much larger storms than tornadoes and cause more economic loss per storm, but tornadoes are typically more intense and they occur more frequently. As late as the 1970's, experts thought tornadoes produced wind speeds in excess of 600 mph and subsequently thought that it was impossible to design a structure to resist tornadic wind loads. Researchers have recently dispelled these myths and have proven that the wind speeds generated by tornadoes range from 80 mph up to 300 mph. Even though the wind speeds in tornadoes can reach velocities approaching 300 mph, over 85% of all tornadoes have maximum wind speeds below 150 mph, (McDonald et al., 1987). This means that normal engineered structures can be economically designed to resist the wind loads generated by over 85% of all tornadoes.

The combined damage resulting from tornadoes, hurricanes, and other wind events have accounted for approximately 70% of all insured losses in the last ten years, as shown in Figure 1.1.

Cumulative Insured Catastrophic Losses
1986 - 1995
(Total Losses $78.5 Billion)

0% — 1%
5%
33%
25%
36%

Legend:
- Other
- Riot/Civil Disorder
- Wind/Hail Tornadoes
- Explosion/Fire
- Earthquake/Fire
- Hurricanes/Tropical Storms
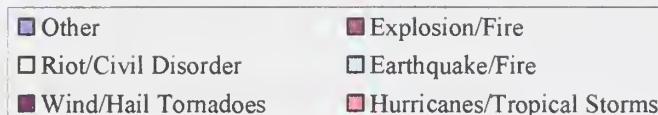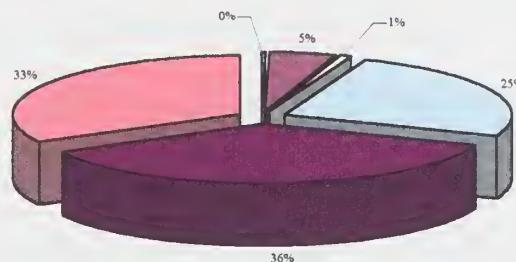
Figure 1.1 Cumulative Insured Losses 1986 to 1995 (PCS, 1996)

Along with their cumulative effects, individual tornadoes and hurricanes can be

devastating. The damage from an individual hurricane can run as high as $30 billion

dollars as it did for Hurricane Andrew in 1992, (Greenberg, 1994). Table 1.1 below,

provides a list of some of the most devastating hurricanes that have hit the United States

in the last 50 years (Palm Beach Post, 1996).

Table 1.1 Most Devastating Hurricanes

Hurricane	Year	Category	Damage (Millions)
Andrew	1992	4	30,000
Hugo	1989	4	7,160
Betsy	1965	3	6,460
Agnes	1972	1	6,420
Camille	1969	5	5,240
Diane	1955	1	4,200
New England	1938	3	3,590
Frederic	1979	3	3,500
Alicia	1983	3	2,390

It is important to note that the damage estimates listed in the previous table have been adjusted to equivalent 1994 dollar values. Although the damage estimates in Table 1.1 and Figure 1.1 include damage to items other than structures, they do give an appreciation for the amount of damage caused by these storms. The extreme damage and loss of life produced by these high wind events has prompted a sub-specialty within civil engineering, called "wind engineering". Through the development of this specialized area and through extensive research, much knowledge has been gained within the last ten years about the loading induced on buildings and other structures by high winds. This report focuses specifically on the performance of low-rise steel structures during medium and high wind events. Through investigation of the performance of actual structures, conclusions can be reached about the adequacy of the current wind codes and construction practices.

Low-rise steel structures can be broadly divided into two main categories, heavy and light steel structures. Heavy steel structures are typically fully engineered buildings that utilize standard American Institute of Steel Construction (AISC) wide flange sections for columns and either wide flange sections or custom designed trusses for beams and girders. Heavy steel structures typically perform well in severe wind events because they are fully engineered and have a high degree of redundancy in the structural systems. Heavy steel structures are enclosed with a number of different types of exterior cladding. Some of the more popular types of cladding are corrugated steel or aluminum siding, normal clay masonry and concrete masonry units (CMU). These exterior claddings and veneers are used both alone, and in combinations.

Light steel structures are typically pre-engineered or partially engineered structures. These light steel structures are usually made up of either single bay rigid frames (such as a standard pre-engineered metal building) or tubular steel columns with standard open web steel joists. The exterior cladding used for these light steel structures is similar to the cladding used for heavy steel structures. Light steel structures typically have little or no redundancy in their structural system, particularly the portions of the system that resist lateral and uplift wind loads. The lack of structural redundancy in these structures is perhaps the single most common cause of their failure during high winds.

1.1 Purpose of the Study

The goal of this forensic engineering study is to objectively evaluate the field performance of low-rise open span heavy steel structures that have been subjected to extreme wind events. The performance of each of the structures studied in this report is evaluated and patterns of failure are noted and analyzed. After the patterns are identified and analyzed, recommendations for improving the performance of these structures are presented. Finally, the report endeavors to either suggest code modifications or recommend areas requiring further study.

1.2 Scope of the Study

As stated earlier, this report examines the performance of open span low-rise heavy steel structures subjected to high wind events. In particular, the strengths and weaknesses of this type of structure are observed and recorded. The information and photographs used in this report were primarily obtained from field investigations of over 70 storm events made by faculty and students working at the Institute for Disaster

Research (IDR) at Texas Tech University. It is important to note that without the countless hours and dedication of the faculty and staff at Texas Tech University, this report would have been impossible to produce.

Building damage and failures resulting from the following high wind events are included in this report: Hurricanes Frederic (1979), Gilbert (1988), Hugo (1989), and Andrew (1992), along with a tornado at Altus, OK (1982). Since these hurricanes and tornadoes subjected many steel structures to the design level wind velocities specified in ASCE 7-95, they provide unique opportunities to objectively evaluate the field performance of these structures.

CHAPTER 2

BACKGROUND

The accurate determination and interpretation of recorded wind velocity information is an important element in the analysis of the damage done by any wind event. To understand and properly interpret the wind velocity information, there are two fundamental concepts about wind flow that must be understood. One concept is that wind velocity varies with height. The second concept deals with the averaging time of a set of anemometer data. A detailed explanation of these two concepts is given in the following paragraphs to provide the background information necessary for understanding the remainder of the material in this report.

Since the velocity of wind varies with the height above ground, it is important to note the recording height of an anemometer reading. The wind speeds are generally lowest at ground level and increase with increasing elevation above the ground. In fact, the wind speed is assumed to be zero at ground level and assymtotically approaches an undisturbed maximum value at a particular height above the ground. This height is called the gradient height and varies depending on the roughness of the terrain and the number and size of the structures in the area. Although the normal distribution of wind speed versus height has been proven to accurately model straight winds, experts are still trying to determine whether it is valid for the distribution of wind speeds in hurricanes and tornadoes. The current theory held by many prominent wind experts is that the wind speed distribution does hold true for hurricanes and tornadoes. This theory is supported by the similarity of the damage patterns produced by all wind events.

As mentioned earlier, the other item that is critical to the understanding and use of reported wind speeds is the averaging time. The averaging time of the wind speed record can have a significant impact on the reported value of any given wind speed. Since wind speeds fluctuate greatly, the reported velocities will be much lower if the averaging time of the sample is increased. This phenomenon is most easily understood by studying an actual wind speed record, such as the one shown in Figure 2.1.
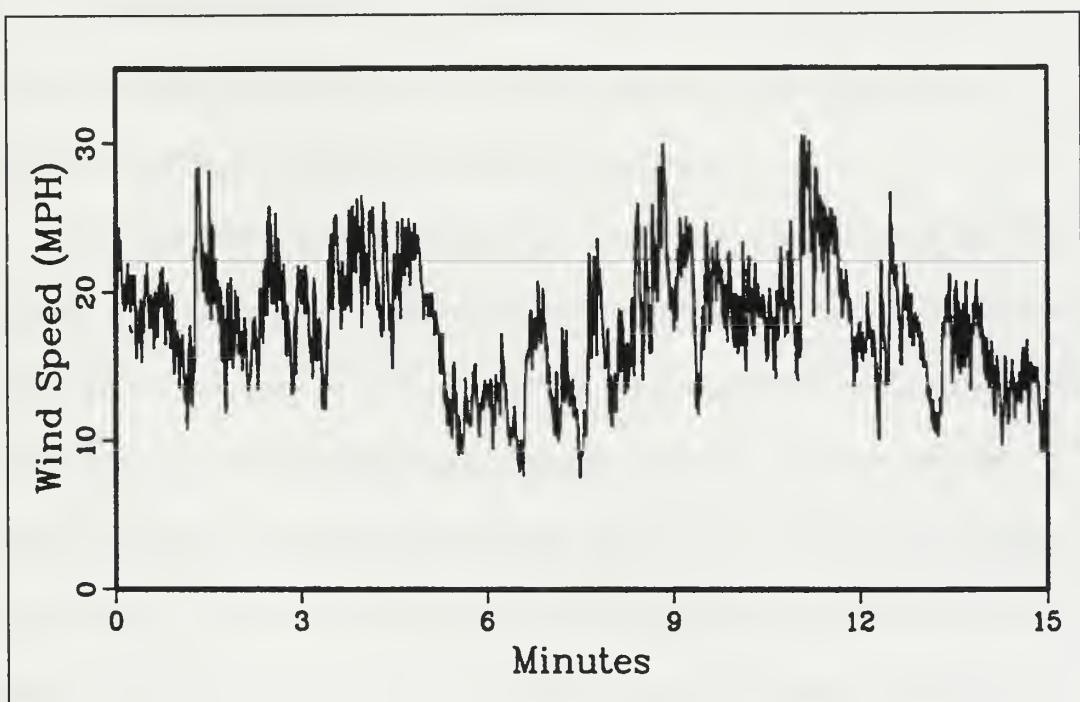
Figure 2.1 Typical 15-Minute Wind Speed Record (Texas Tech WERFL Site)

If a three second averaging time is chosen, the maximum wind speed reported for the record shown in Figure 2.1 would be close to 30 mph. If a three minute averaging time is chosen, the reported wind speed would be approximately 22 mph, which is an average of the wind speed records between 9 and 12 minutes. As shown by this example, the maximum average wind speed reported for a given set of data can vary greatly depending

7

on the averaging interval. An accurate comparison of wind speeds from different storms can only be made if the reported maximum wind speeds are obtained at the same height, using the same averaging time. If all reporting conditions are not the same, conversions must be made to make a comparison of the data meaningful. Since the prevailing wind standards now use the maximum sustained three second gust recorded at 33 feet (10 meters) above ground level as the standard, all wind speeds presented in this paper have been converted to this standard. The conversions were made using the logarithmic law as recommended by Simui and Scanlan, 1996. The equations for the logarithmic law along with the conversion calculations are included in Appendix A.

The high wind events mentioned in this report are categorized using the Saffir-Simpson Scale for hurricanes and the Fujita Scale for tornadoes. Both the Saffir-Simpson and the Fujita Scales provide a means of quickly rating and comparing the strength of a hurricane or tornado. While tornadoes are primarily rated by an assessment of the damage they produce, hurricanes are rated based primarily on maximum wind speed. Along with the maximum wind speed, the Saffir-Simpson scale uses the height of the tidal surge to categorize hurricanes. The Saffir-Simpson scale ranks the strength of a hurricane on a scale of one to five and is broken down as shown in the following table.

Table 2.1 Saffir-Simpson Hurricane Scale

Category	Wind Speed (Mph)	Tidal Surge (ft)
1	74 – 95	4 – 5
2	96 – 110	6 – 8
3	111 – 130	9 – 12
4	131 – 155	13 – 18
5	>155	>18

It is important to note, that the averaging time and sampling height of the wind speed data used in the Saffir-Simpson scale are not specified (Simiu et al., 1996). Since these parameters are necessary for the use of the wind data in structural calculations, the Saffir-Simpson scale can only be used as a qualitative measurement of hurricane intensity.

The Fujita scale, which was developed to categorize the intensity of tornadoes, is broken into six different levels. Each level describes a particular degree of damage. Only in recent years have corresponding wind speeds been assigned to the Fujita scale. The Fujita scale is broken down as shown in Table 2.2.

Table 2.2 Fujita Tornado Scale

Category	¼ Mile Wind Speed (Mph)	3 Second Wind Speed (Mph)	Damage
0	40 – 72	45 – 78	Light
1	73 – 112	79 – 117	Moderate
2	113 – 157	118 – 161	Considerable
3	158 – 206	162 – 209	Severe
4	207 – 260	210 – 261	Devastating
5	261 – 318	262 – 317	Incredible

The averaging time for the Fujita scale is specified. The Fujita scale uses the maximum one-quarter mile wind speed for its standard. The one-quarter mile wind speed is fastest average wind speed obtained for a quarter of a mile of wind passing an anemometer. Both the one-quarter mile and the three second gust wind speeds are given in Table 2.2. It is important to note that the categories in the Saffir-Simpson and the Fujita scales are used in the following chapters only to describe the relative intensity of the high wind events that affected the subject structures.

2.1 Evolution of the United States Wind Load Standard

The first modern standard for the calculation of wind loads on structures was published by the American National Standards Institute (ANSI) in 1972 and was designated ANSI A58.1-1972. Along with the wind load provisions in this standard, it also included the minimum design criteria for dead loads, live loads, snow loads, rain loads and earthquake loads. However, due to ambiguities and inconsistencies in the terminology used in the section of the standard that governed wind loading, it never gained widespread acceptance, (Mehta et al., 1991). In 1976 a cross-functional, 46 member committee was established to revise the wind provisions of the ANSI A58.1-1972 standard. This committee was established following a conference at Northwestern University where valuable input was obtained from practicing engineers, building code representatives, and industry personnel. The 46 member committee revamped the wind provisions of the 1972 standard and published a revised edition of ANSI A58.1 in 1982. Three major improvements were made in this revised standard. First, much of the ambiguous language was clarified. Second, the new standard included codified criteria requiring designers to account for the high localized pressures produced at areas of flow separation. The final improvement made to the standard was the introduction of a new design velocity contour map. The revised contour map was based on fastest mile wind velocities obtained at 33 feet instead of 30 feet, as was used for the 1972 map. The change to the maximum wind speed obtained at 33 feet above the ground surface increased the design velocities in many areas. These three major changes made ANSI A58.1-1982 the first standard that was widely accepted in the United States for the calculation of wind loads on structures.

The responsibility for the A58.1 wind code was transferred to the American Society of Civil Engineers (ASCE) in 1985. After minor revisions, the ASCE published a new standard, ANSI/ASCE 7-88, in 1990. This revised version of ANSI A58.1-1982 and especially the commentary on the use of the wind load provisions were a great improvement over the old standard. The revised standard provided a better format, consolidating all of the wind provisions and charts in one section. The commentary provided background information on the development of the wind provisions so the practicing engineer could get a quick explanation of the basis of the provisions along with a more in-depth explanation of how to interpret the standard. In 1993, the wind sub-committee further refined the ASCE wind standard and published ASCE 7-93. Virtually no substantive changes were made to the wind provisions in the ASCE 7-93 standard. In 1995, the wind sub-committee again revised the wind standard and published ASCE 7-95. ASCE 7-95 is the current standard that is used today. The primary change in the ASCE 7-93 standard was a revised design wind velocity map. In the new map, the wind subcommittee used a maximum three second gust instead of the fastest mile wind speed that had been utilized in all codes prior to ASCE 7-95. Even though the use of the three second gust resulted in higher design velocities, the design wind loads on the majority of the structures did not change significantly due to modifications to the pressure coefficients in the ASCE 7-95 standard. The differences between the two standards can be readily seen by comparing the design wind velocity contour maps from ASCE 7-88, which is identical to the 7-93 map, and ASCE 7-95. The velocity contour maps from these standards are shown in Figures 2.2 and 2.3.
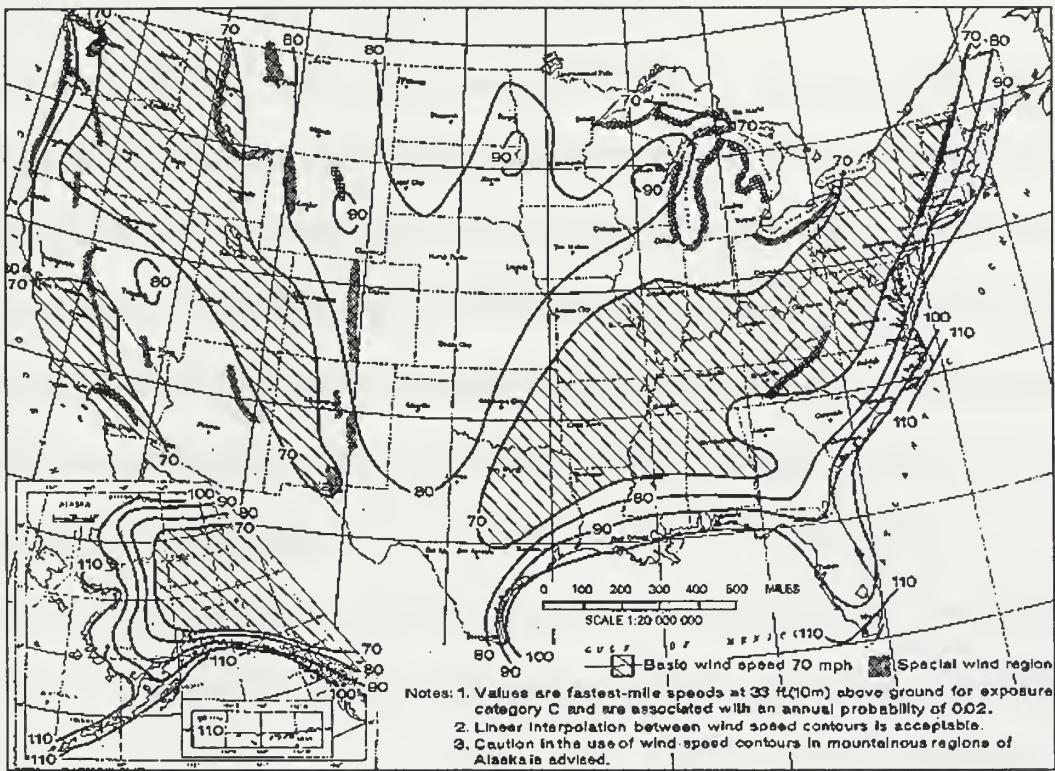
Figure 2.2 Design Wind Velocity Contour Map - ASCE 7-88
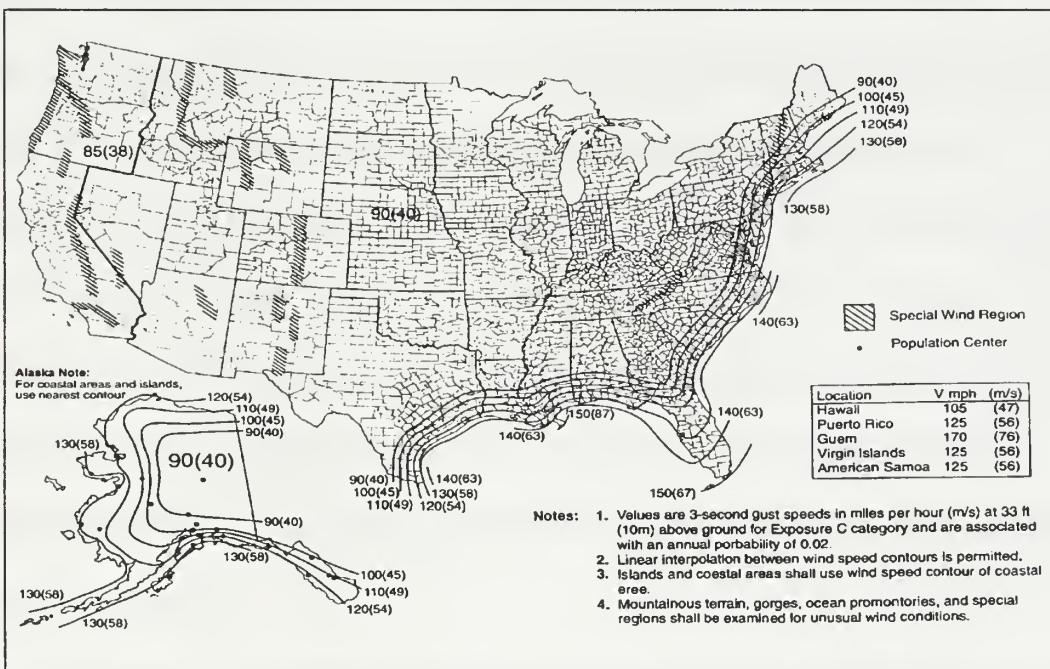
Figure 2.3 Design Wind Velocity Contour Map - ASCE 7-95

2.2 Methods of Analysis

One of the most difficult tasks to accomplish when conducting an engineering investigation of storm damage is obtaining a reliable estimate of the wind speeds that caused the damage. Over the years, engineers have developed four main ways to estimate the wind speeds generated by a storm. The first method is to analyze the damage done to residences and rural buildings, by wind generated missiles. Because of the wide range of construction practices used to build these structures and the dynamic complexities involved with missile impacts, this type of analysis provides estimates that are questionable (Mehta, 1976). The second method is the analysis of framed structures or conventional buildings that have been damaged or destroyed. Again because of variation in construction techniques and materials, this method provides estimates that are only acceptable (Mehta, 1976). The third method used is a detailed analysis of "simple" structures that have either been damaged or have failed. Some examples of these "simple" structures include signs, light poles, single column canopies, bridge beams, and towers. Since the structures are very simple, the analysis typically provides good estimates of wind speeds (Mehta, 1976; Marshall et al., 1983). The fourth method is to obtain wind speed records from anemometers that were located in the path of the storm. This method provides excellent confidence in the reported values, but unfortunately, this data is normally not available. Even when the data is available, it must be carefully validated and the height and averaging time must be converted to standard values before the data can be used.

Since many of the structures that are studied in this report were located on military installations or close to airports, reliable direct anemometer readings were readily

available. The only problem with direct anemometer data is that the averaging times, exposure conditions, and sampling heights sometimes vary. As stated in the background discussion of this chapter, all the wind speeds reported in this report are for a three second gust on open ground at a sample height of 33 feet (10 meters). The anemometer data that did not conform to this standard was converted using the equations and methods recommended by Simiu and Scanlan, 1996.

Where reliable data was not available, wind speeds were estimated based on the loads required to cause the failure of "simple" adjacent structures. The analysis of these simple structures was performed in accordance with the general wind load provisions of Section 6 of ASCE 7-95 and can be found in Appendix A. Along with the analysis of the "simple" structures, the wind load provisions of Section 6 of ASCE 7-95 were also used for the analysis of loads on the structures studied in this report. The general equation used to calculate the wind loads on the structures is provided below.

$$q_z = 0.00256*K_z*I*V^2$$

q_z = velocity pressure evaluated at height z, in pounds per square foot (psf)
K_z = wind pressure exposure coefficient evaluated at height z
I = importance factor of the structure
V = basic design wind speed (mph)

Once q_z is obtained, it is used to calculate the design wind pressure, p. The design pressure is calculated using q_z, and several coefficients that account for the specific conditions of the site and the properties of the building. Some of the coefficients that account for the site conditions include a gust effect factor, internal pressure coefficients, and external pressure coefficients. The design pressure is then multiplied by the projected area normal to the wind direction to obtain the wind loading.

CHAPTER 3

METEOROLOGICAL INFORMATION

The meteorological information in this section is provided to add meaning to the damage discussed in the next chapter. The meteorological information about the storms was obtained from the Purdue University Atmospheric Sciences database via the Internet. The origin, path, and the strength of each storm is provided to give an indication of the wind speeds and storm direction at each of the damage sites studied. Along with this specific information about the individual hurricanes, it is also helpful to understand the general principles of the formation and growth of hurricanes.

Hurricanes are formed when a cool moist air mass passes over a warmer body of water. As the moist air mass passes over the warm water, the air mass absorbs moisture and the air begins to spin, thus forming a column and a tropical depression. As additional moist air rises and strengthens the storm, the entire air mass surrounding the column begins to travel in a circular motion around the column. This process continues as long as the system is supplied with a large body of warm water and as long as the temperature differential between the water and the air mass is maintained. The storm is classified as a hurricane when the parameters in Table 2.1 are met.

All of the hurricanes that caused the subject damage began as tropical depressions at various locations in the Atlantic Ocean and made landfall in the southern or southeastern United States. Detailed information on each of the hurricanes is described later in this chapter. The hurricanes are discussed in chronological order with no regard to the severity of the damage or intensity of the storm. The following color scheme is

used to represent the severity of the hurricanes in Figures 3.1 to 3.5: Green - tropical depression, yellow - tropical storm, red - category 1 hurricane, light red - category 2 hurricane, magenta - category 3 hurricane, light magenta - category 4 hurricane, and black - category 5 hurricane. The stars on the hurricane tracking maps indicate the approximate location of the damaged structures.

3.1 Hurricane Frederic

Hurricane Frederic began as a tropical depression on August 29, 1979 at latitude 11° North and longitude 25° West. Frederic's initial position was approximately 2,500 miles east of the north end of South America. The storm took a westerly course and strengthened slightly as it moved toward the Caribbean. Before it reached tropical storm strength, it made landfall on various islands in the Caribbean. After continuing its easterly track and clearing Cuba, it quickly turned north and headed toward the Mississippi-Alabama border. When it made landfall on September 12, 1979 between Pascagoula, Mississippi and Mobile, Alabama, it had reached category 4 strength. For the purposes of this report, the area of interest is near Mobile, Alabama. The eye of Hurricane Frederic passed less than 100 miles to the east of Mobile. Maximum wind speeds of between 100 and 110 mph were recorded by the National Weather Service (NWS) at the Mobile Airport and by the Coast Guard Cutter, Salvia when Frederic passed over Mobile (Mehta et al., 1981; Reinhold, 1979). An illustration showing the track of this hurricane and its corresponding strength can be seen in Figure 3.1.
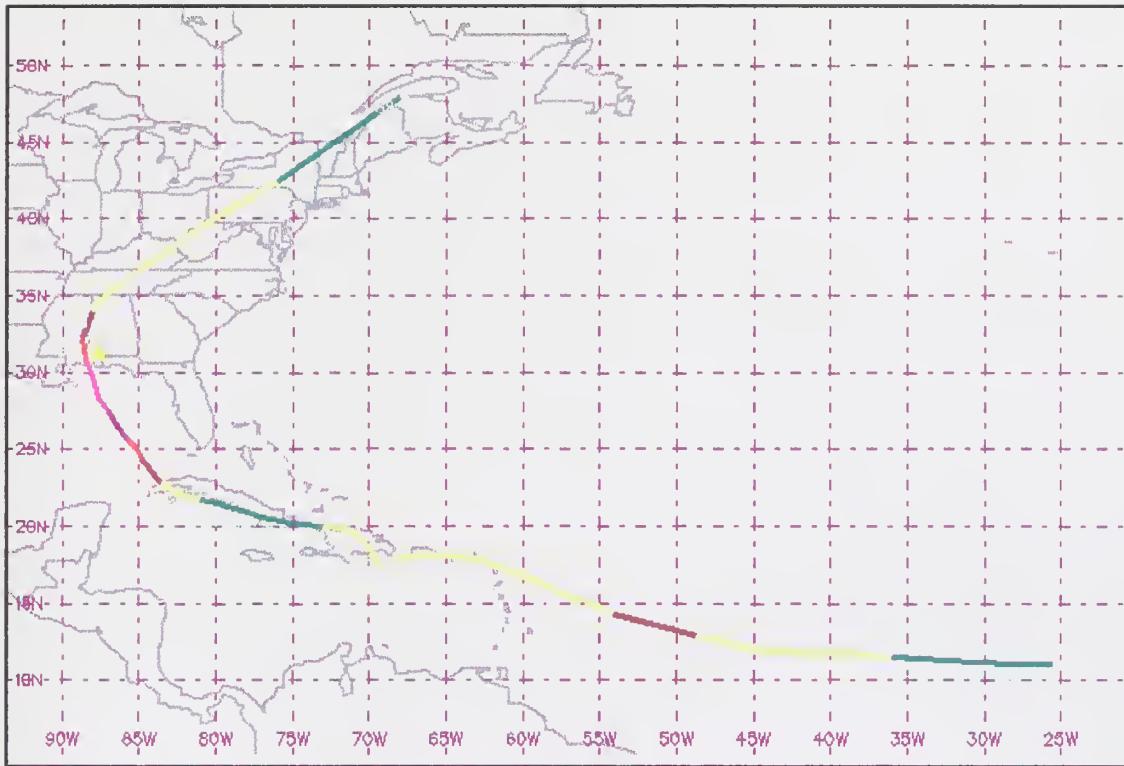
Figure 3.1 Tracking Map for Hurricane Frederic

3.2 Hurricane Gilbert

Hurricane Gilbert began as a tropical depression on September 8, 1988 at latitude

12° North and longitude 54° West. Gilbert's initial position was approximately 500 miles

east of the north end of South America. The storm took a west to northwesterly course

and strengthened to a category 3 hurricane before making landfall on the Caribbean

island of Jamaica. It then strengthened to a category 5 hurricane as it crossed the

Caribbean Sea and made landfall on the southern portion of the Yucatan Peninsula.

Gilbert weakened to a category 3 hurricane as it crossed the southern tip of Mexico but

gained strength to category 4 as it entered and crossed the Gulf of Mexico. By the time

the storm entered the United States through the southwestern border of Texas, it had

weakened to a tropical depression. Although the continental United States did not
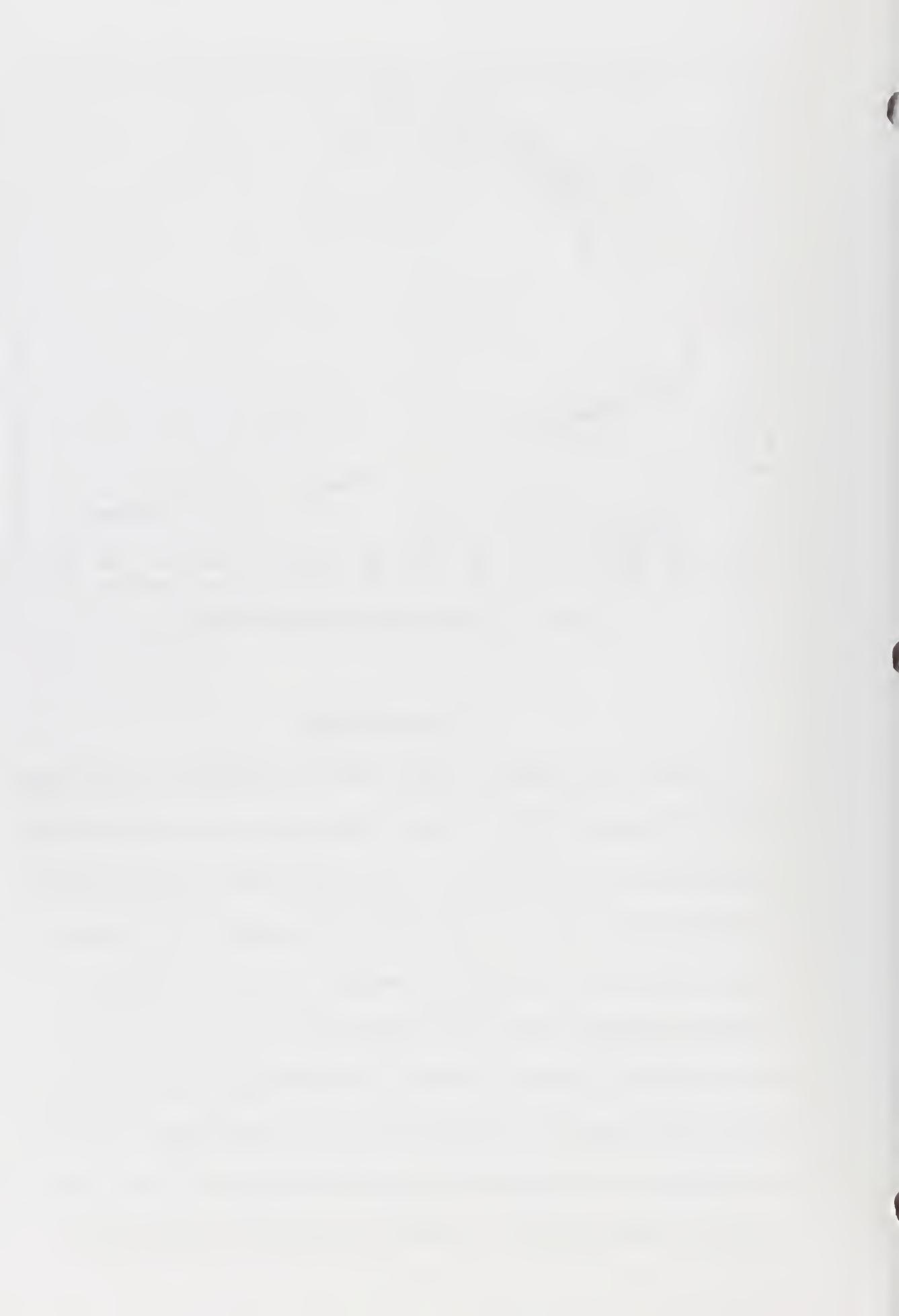
receive much direct damage from Hurricane Gilbert, it spawned a number of tornadoes that caused considerable damage in the South Texas area. One of these tornadoes caused the damage to the structures that were investigated in this report. These structures were located on Kelly Air Force Base (AFB) in San Antonio, Texas, which is over 200 miles away from the path of the hurricane. An illustration of the track of this hurricane and the location of Kelly AFB can be seen in Figure 3.2.
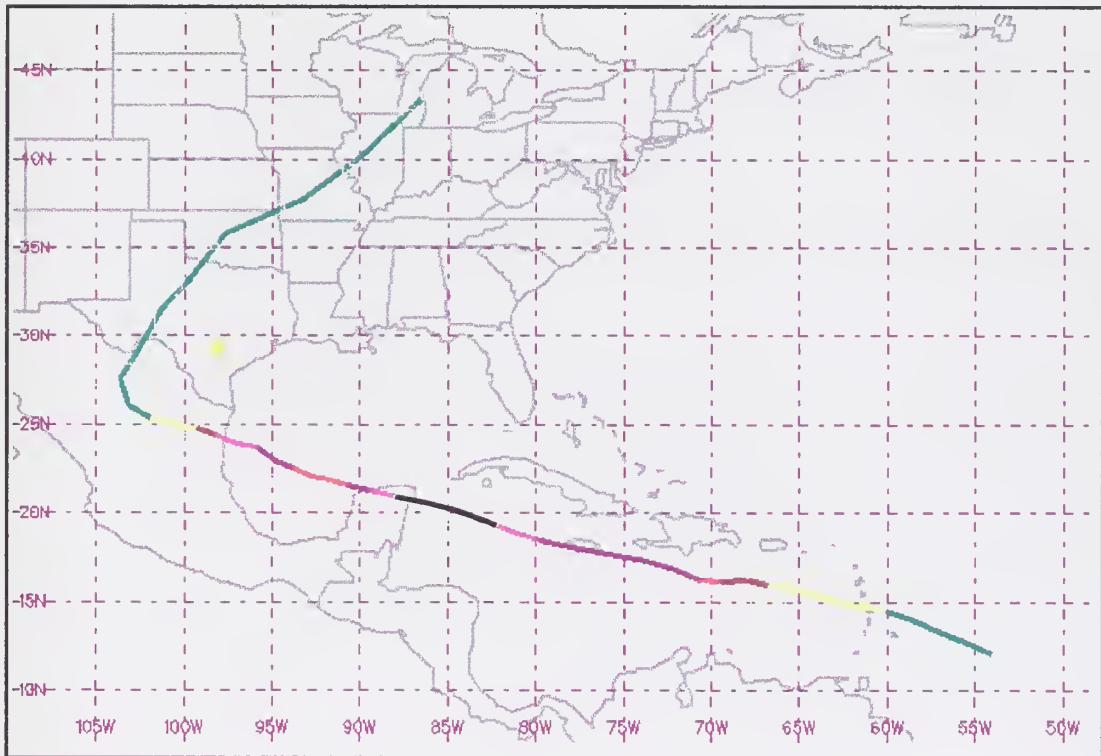

Figure 3.2 Tracking Map for Hurricane Gilbert

3.3 Hurricane Hugo

Hurricane Hugo began as a tropical depression on September 10, 1989 at latitude 13° North and longitude 20° West. Hugo's initial position was approximately 300 miles west of Sengal, Africa. The storm took a westerly course and gained strength as it moved toward the Caribbean. As the storm entered the Caribbean, it turned to the North and headed directly for Puerto Rico. When the storm made landfall on Puerto Rico it had reached category 4 strength. The storm continued on a northwest track and its strength fluctuated between category 3 and 4, as it approached the United States. When Hugo made landfall near Charleston, South Carolina, it was a strong category 4 hurricane. The damage investigated in this report occurred at the Charleston Air Force Base. An illustration showing the approximate location of the Charleston AFB and track of this hurricane can be seen in Figure 3.3.
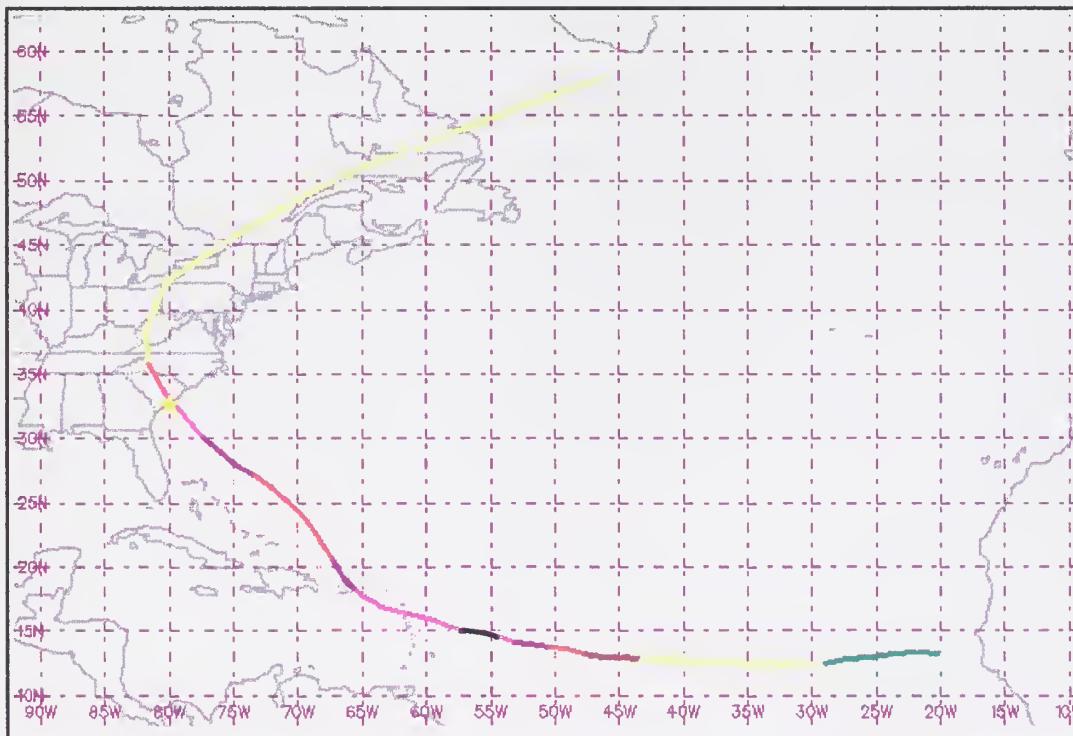
Figure 3.3 Tracking Map for Hurricane Hugo

3.4 Hurricane Andrew

Hurricane Andrew began as a tropical depression on August 16, 1992 at latitude $11°$ North and longitude $35°$ West. Andrew's initial position was approximately 1,500 miles east of the north end of South America. The storm took a northwesterly course and strengthened steadily as it moved toward the Florida coastline. It reached category 4 strength before it first made landfall on the southern tip of Florida. As it moved across Florida, it lost strength down to a category 3 hurricane before entering the Gulf of Mexico. After entering the Gulf of Mexico, Andrew again gained strength and turned north toward Louisiana. When the storm struck Louisiana about 100 miles west of New Orleans, it had again reached category 4 strength. After making landfall, the storm quickly turned to the East and lost strength, dissipating entirely before reaching North Carolina.

The damage investigated in this report occurred as Hurricane Andrew passed over the southern tip of Florida. The location of the approximate location of the damage is indicated on Figure 3.4. The track of Hurricane Andrew and its corresponding strength can also be seen in Figure 3.4.
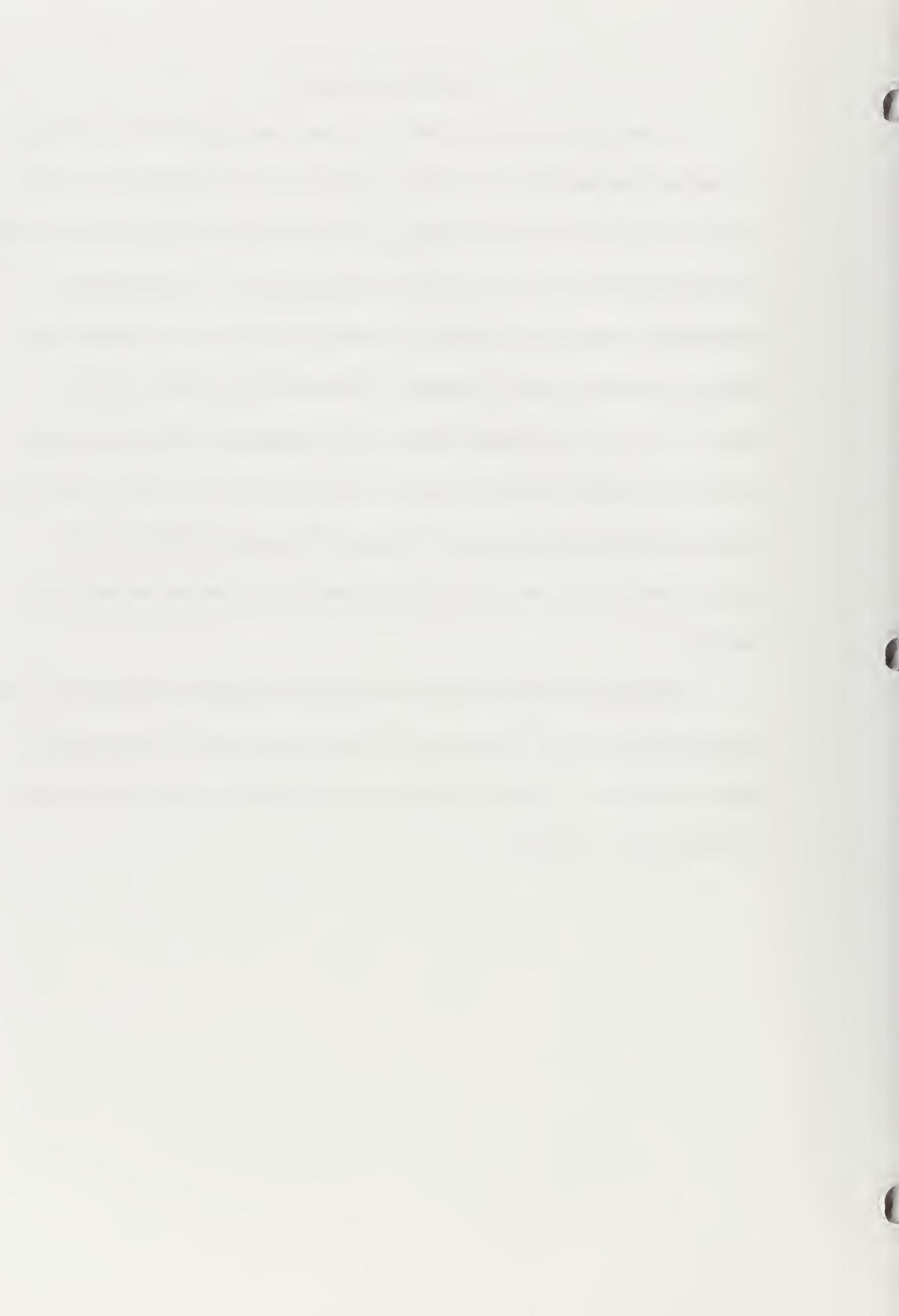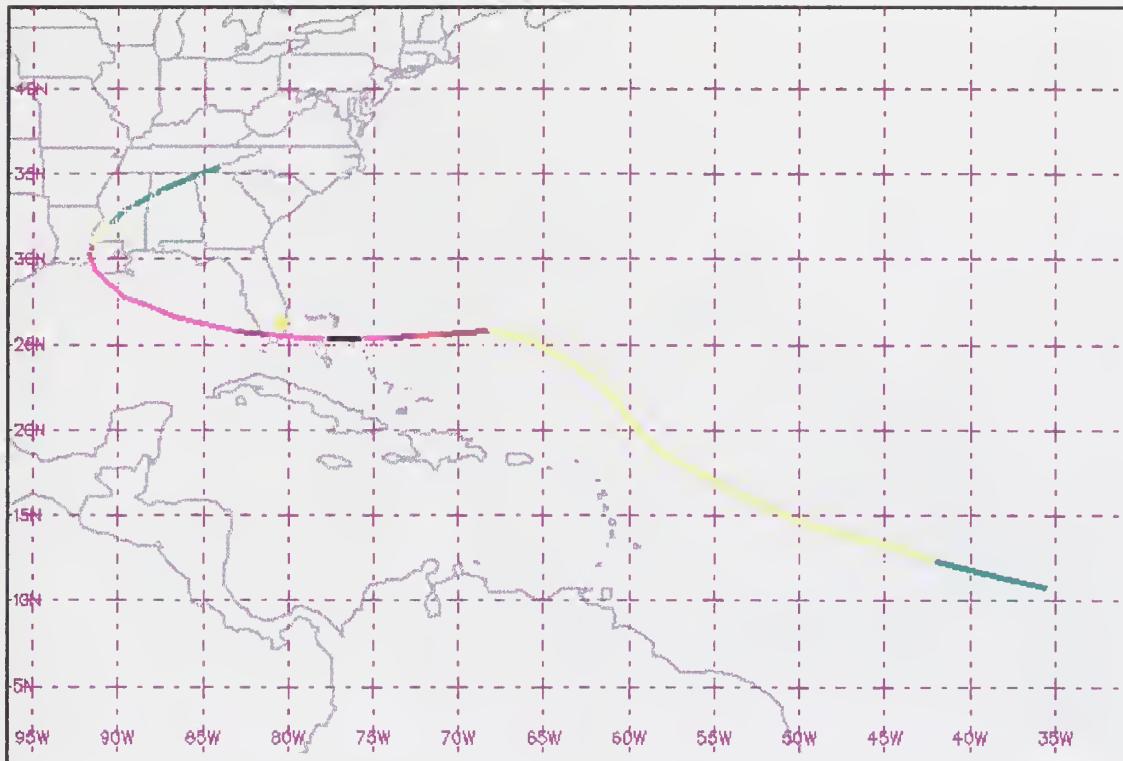
Figure 3.4 Tracking Map for Hurricane Andrew

3.5 Altus, Oklahoma Tornado

Along with the hurricanes mentioned above, there was also a tornado that caused

damage to several low rise steel structures in Altus, Oklahoma. The tornado touched

down on the southwest side of Altus Air Force Base on May 11, 1982. The tornado

traveled northeast across the base and dissipated as it reached the northeast perimeter.

The tornado was estimated to be approximately 1600 feet wide and the maximum

strength was classified as F3 (McDonald et al., 1983). An illustration showing the

strength of the storm and its path is provided in Figure 3.5, on the following page

(McDonald et al., 1983). Of particular note are buildings 279 and 285, both of which are

located approximately 650 feet east of the central path of the tornado.
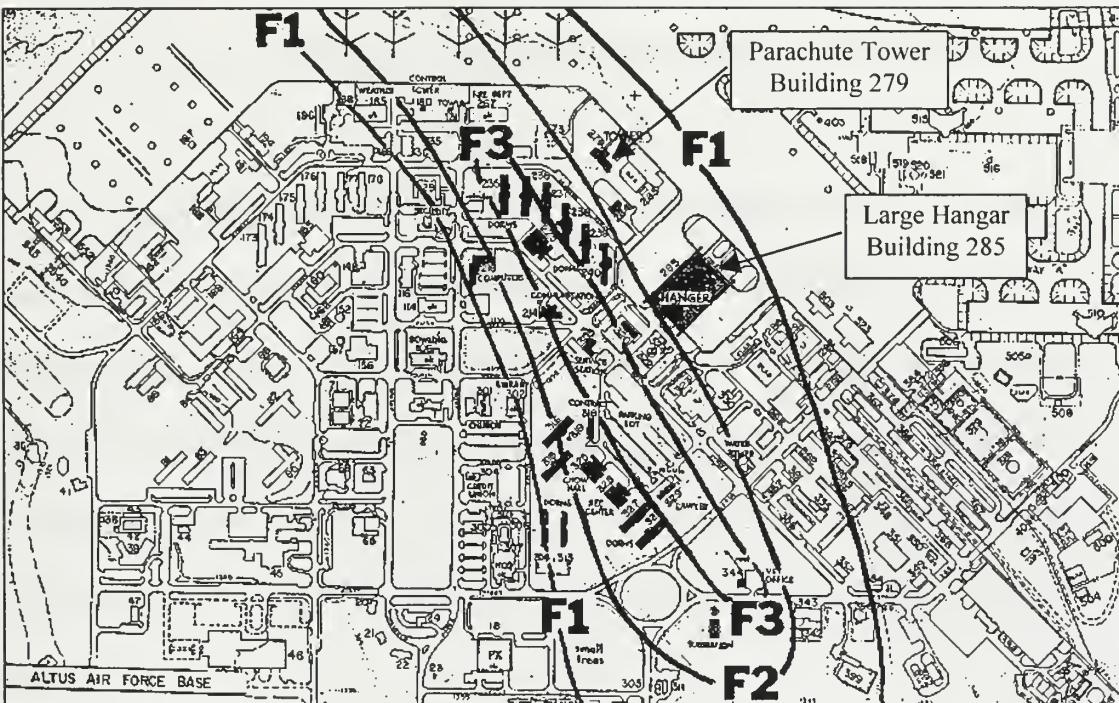
Figure 3.5 Tornado Damage Path Through Altus Air Force Base

CHAPTER 4

BUILDING DAMAGE: DOCUMENTATION AND ANALYSIS

As mentioned earlier, all of the damage documentation for the case studies

presented in this chapter were obtained from the Texas Tech Institute for Disaster

Research (IDR) archives. The case studies discussed in the following sections provide a

representative sample of the damage documented. Although numerous case studies are

available in the IDR archives, the examples provided in this chapter were chosen because

they best represent both the scope and type of damage that was observed on low-rise

heavy steel structures.

4.1 Hurricane Frederic: Building 3

Location and Site Conditions

The subject structure is a large supply warehouse located on a canal that branches

off Mobile Bay. Mobile Bay is located on the east side of Mobile, Alabama. The area

around the site can be generally classified as an open area, exposure C as defined in

ASCE 7-95.

Description of Structure

The supply warehouse is approximately 70 feet wide and 120 feet long. The

columns are standard wide flange steel shapes and are approximately 35 feet tall. Custom

designed open web joist girders run parallel to the short side of the building and attach

directly to the three wide flange columns placed in lines parallel with the short side of the
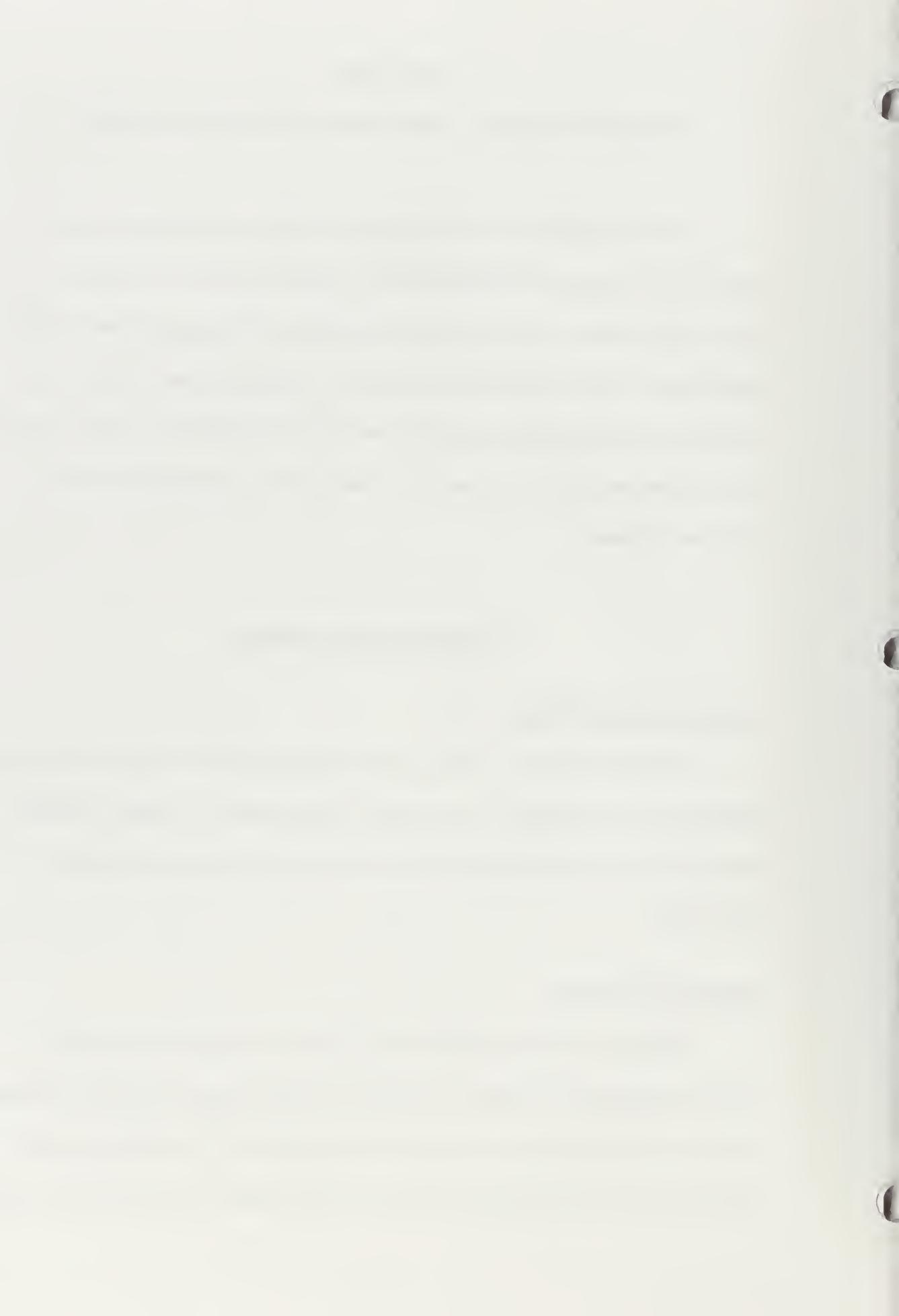
building. The joist girders are spaced approximately 30 feet apart going down the long side of the building. Smaller standard open web joists run perpendicular to the main joist girders. The exterior cladding and roofing consists of corrugated metal siding of an unknown thickness and pattern.

Wind Speed Analysis

The large supply building was damaged by Hurricane Frederic in September of 1979. Although wind direction can shift during the course of a hurricane, the winds were generally coming from the southwest. Reliable anemometer data was available from a NWS site at the Mobile Airport and from the Coast Guard Cutter Salvia. Both of these anemometers were located within 3 miles of the structure. The maximum wind speeds recorded at these stations varied between 100 mph and 110 mph depending on the recording site chosen (Reinhold, 1979). The reliability of this wind speed data is excellent and it generally agrees with the hurricane tracking chart that was shown previously in Figure 3.1.

Description of Damage

This warehouse building sustained no significant structural damage, as can be seen in Figures 4.1, 4.2, and 4.3. The only damage noted was the failure of several large overhead doors and the removal of some of the corrugated metal roof and wall panels.

Analysis of Damage

The probable cause of the roof and wall panel failure was the prior failure of the large overhead doors located on the side of the building running parallel to the railroad tracks, as seen in Figure 4.1. These overhead doors failed due to positive pressure

generated by wind blowing normal to the surface of the doors. Once the two overhead doors failed, the internal pressure inside the building increased and the roof panels and siding were torn from the structure due to the combined internal and external pressure.

Points of Interest

There are several important points to note in the damage done to this structure. First, there was little or no damage done to the steel framing and girts supporting the overhead doors. This indicates that either the door curtain had insufficient structural capacity to transfer the wind load to the frame, or that the door tracks deflected enough to allow the curtain guides to separate from the tracks. Regardless of the mechanism, the failure of these and other overhead doors has been observed repeatedly in other structures that sustained damage.

The second point to notice is the lack of damage to any of the wall girts or roof joists that supported the damaged panels. The lack of damage to the girts and joists can be attributed to a combination of the small vertical spacing of the girts, approximately three feet, the use of heavy "C" channel sections, and the premature failure of the corrugated siding. It is important to note that since the siding failed, the girts were probably not subjected to the maximum wind loads.

The last item to notice is the mode of failure of the corrugated panels. Since the screws remained in the girts after failure, this indicates that either the fastener spacing was too large, the heads of the fasteners were too small, or the thickness of the corrugated siding was insufficient to prevent the corrugated siding from experiencing localized failure around the screws.

25

Figure 4.1 South Exterior Elevation of Building 3



Figure 4.2 West Exterior Elevation of Building 3

Figure 4.3 Interior Elevation of Building 3

4.2 Tornado at Altus, Oklahoma: Building 279

Location and Site Conditions

Building 279 is the designation for both a standard low rise wood frame structure and a separate parachute drying tower. Both of these structures are located just east of building 285 on Altus AFB, as shown previously in Figure 3.5. The structure of interest is the parachute drying tower. The parachute drying tower is a free standing structure located adjacent to the northeast corner of building 279. The area around building 279 is generally unobstructed and classifies as open terrain, exposure C, as defined by ASCE 7-95.

Description of Structure

The parachute drying tower is a steel frame structure that is 15'-6" wide, 28'-6" long, and 62'-4" tall. The tower has four wide flange steel columns and various wide flange beams. A plan view of the structure can be seen in Figure 4.4. The tower is structurally braced against sidesway by double angles that are attached to the four columns at intermediate levels as shown in Figures 4.5 and 4.6. These cross braces transfer the lateral loads into the columns and the columns transfer the loads into the foundation via base plates and four 5/8" diameter A307 bolts as shown in Figure 4.7. The exterior walls of the tower are covered with corrugated asbestos siding.

Since the parachute drying tower is a very "simple" structure, the analysis of the failure of this structure provides a good estimate of the wind speeds generated by the tornado. The main reason for the inclusion of the tower failure in this report is to provide a valid estimate of the wind speed that caused damage to building 285. Building 285 is a

heavy steel structure that was also damaged by the Altus tornado and will be discussed in detail in the next section. Building 285 is located approximately 600 feet from the tower. Although Building 285 is located 600 feet from the tower, both structures are in a line that is parallel to the path of the tornado and thus they experienced approximately the same wind speeds. The location of the two structures can be seen in Figure 3.5, as mentioned previously.
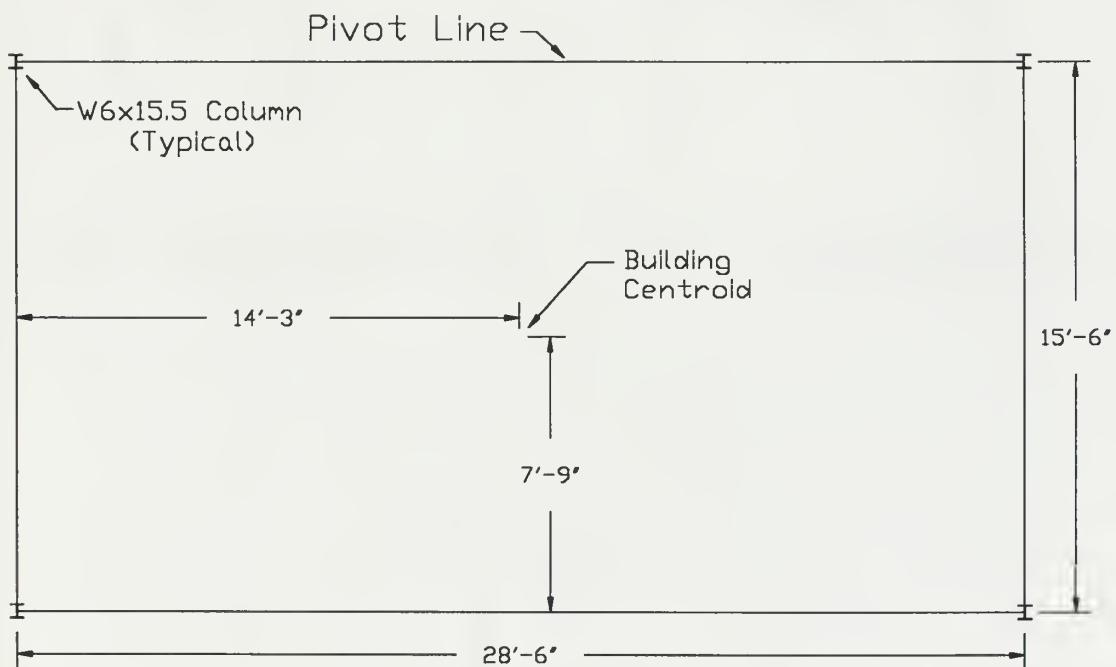
Figure 4.4 Drawing, Plan View of Parachute Tower
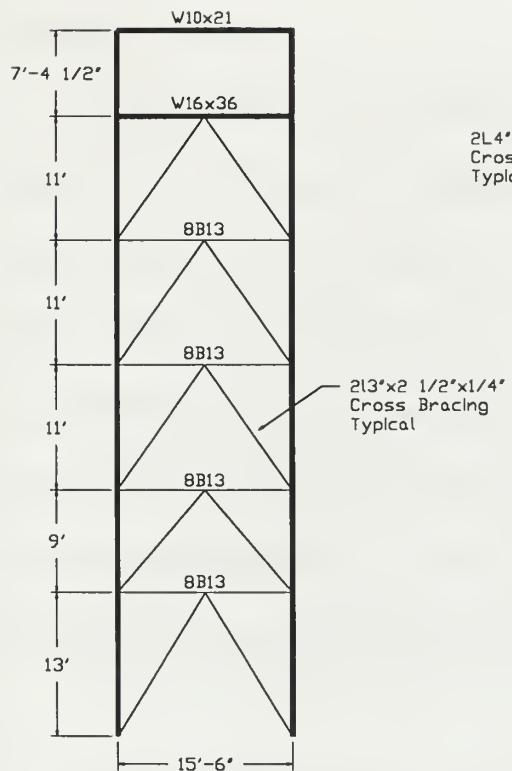
Figure 4.5 Drawing, Parachute Tower
East Elevation

Figure 4.6 Drawing, Parachute Tower
South Elevation
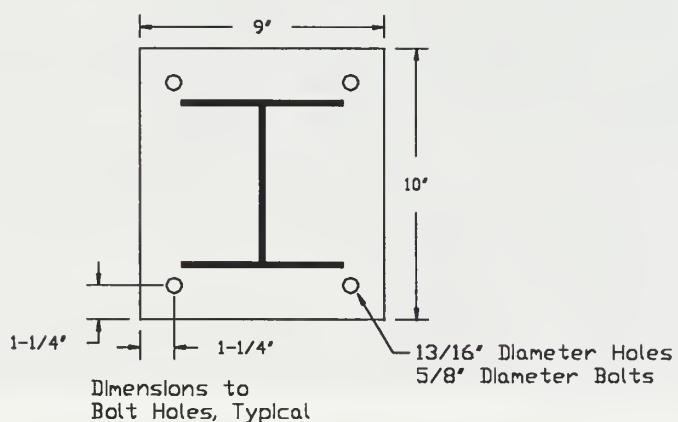
Figure 4.7 Drawing, Parachute Tower Column Base Plate

<u>Description of Damage</u>

As seen in Figure 4.8, the parachute drying tower was totally destroyed by the Altus tornado. The failure of the tower was caused by excessive wind loads on the windward and leeward walls. These wind loads were sufficient to cause the anchor bolts on the southeast and northeast columns to fail in tension. Once the anchor bolts failed, the overturning moment generated by the easterly wind caused the building to rotate about the other two columns and collapse. A close up of the anchor bolt failure can be seen in Figure 4.9 and a close up of the column base plate in Figure 4.10. Figure 4.10 shows definitively that the base plate did not fail.

Figure 4.8 Failure of Parachute Tower
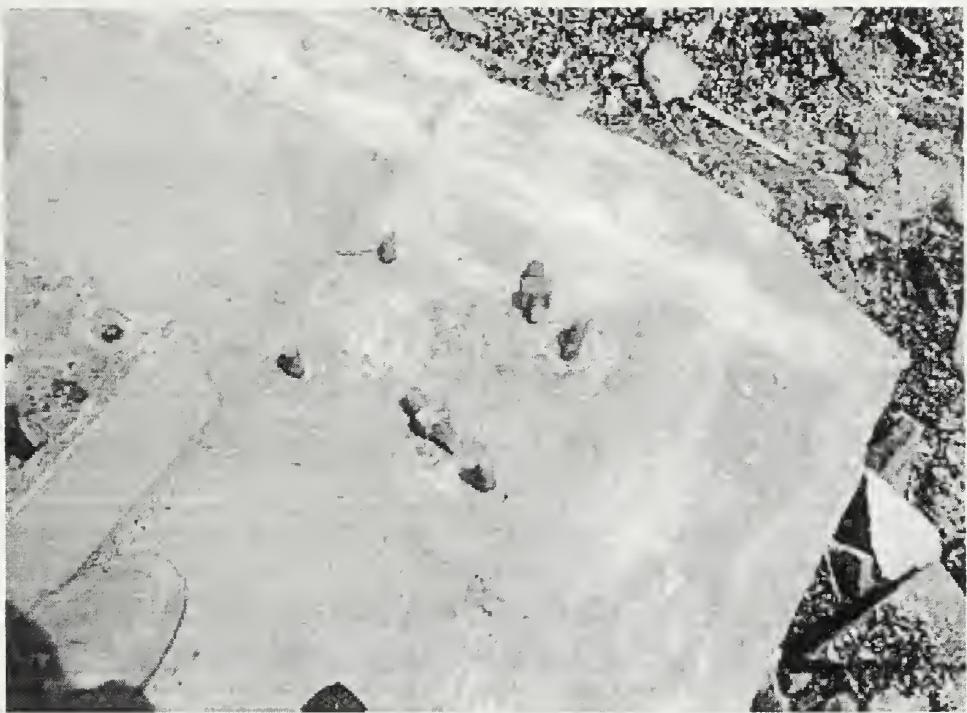
Figure 4.9 Anchor Bolt Failure, Parachute Tower

Figure 4.10 Column Base Plate, Parachute Tower

Analysis of Wind Speed

The wind that caused the collapse of the parachute tower was generated by the Altus, Oklahoma tornado that was described earlier in Section 3.5. The wind caused the collapse of the parachute tower by generating enough force to cause failure of the column anchor bolts and also overcome the righting moment generated by the weight of the building. An illustration of the forces acting on the structure can be seen in Figure 4.11, below.
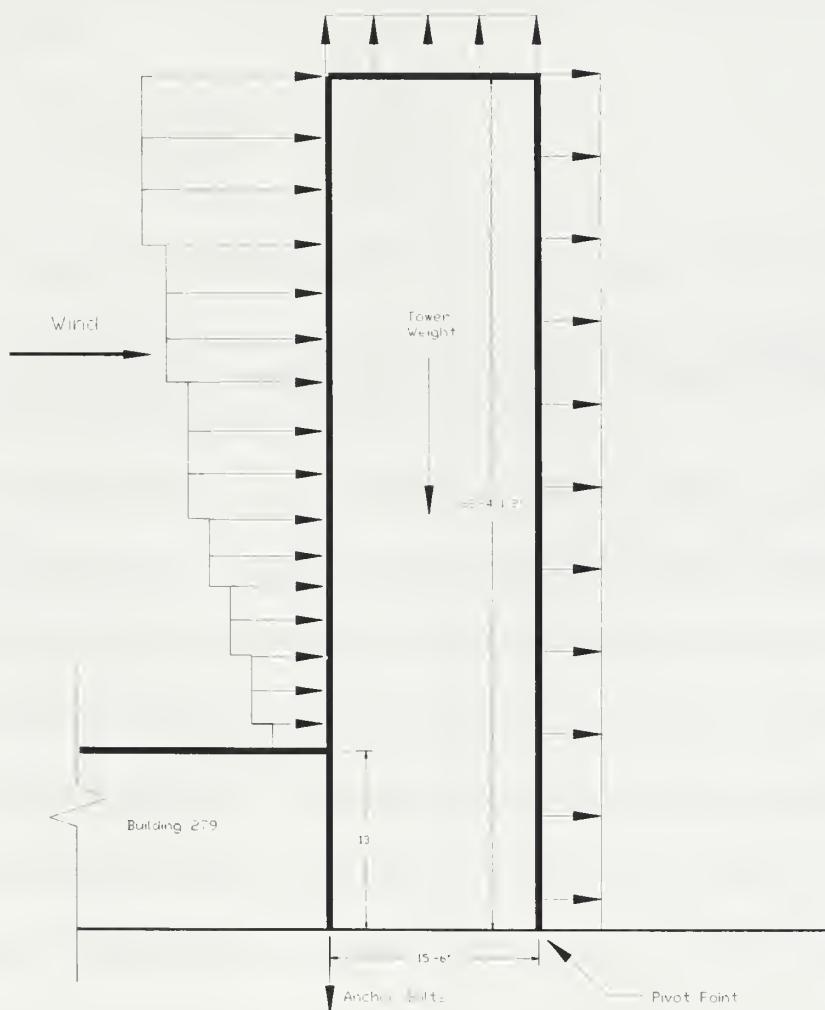
Figure 4.11 Forces Acting on Parachute Tower

An estimate of the wind speed necessary to cause the failure of the tower was determined using the following conditions and assumptions:

1. The wind pressure varied over the height of the tower according to the distribution pattern shown in ASCE 7-95.

2. The maximum static wind load acted normal to the longest dimension of the building in plan view.

3. The stress in the four A307 anchor bolts was equal prior to failure.

4. The atmospheric pressure changes did not appreciably contribute to the collapse of the structure.

5. The external pressure coefficients acting on the building surfaces are as follows:

Windward wall	$C_p = 0.8$
Leeward wall	$C_p = -0.3$
Roof	$C_p = -1.3$

6. The gust effect factor applied to the external pressure coefficients is .86.

7. The total weight of the structure was 67,269 pounds. This weight was calculated from as-built drawings of the tower. Detailed information on these calculations can be found in Appendix A.

The assumption that the wind velocity on the windward side of the structure varies with the height of the structure is consistent with ASCE 7-95. Although some literature suggests that the wind speed in tornadoes does not vary appreciably with height, no concrete proof of this theory exists. Assumptions two and three are fairly obvious and require no additional explanation. Assumption four is substantiated by investigations of other tornado damage by McDonald et al., 1987. Since no other concrete theory exists to warrant the use of other exposure coefficients, the ones found in ASCE 7-95 were used. Assumption six is an adjustment that was made to the normal gust factor of .85, recommended in ASCE 7-95. The gust factor was calculated using the complete analysis

equations given in the commentary of ASCE 7-95. The complete analysis was used to account for any increase in the gust effect factor caused by the slenderness of the parachute tower. The equations and the detailed calculations used to obtain the gust factor can be found in Appendix A. Once these assumptions have been made and justified, the calculation of the maximum wind velocity proceeded as shown in the following paragraph.

The load capacity of one of the anchor bolts, ϕR_n, is defined by the following equation (AISC, 1995).

$$\phi R_n = \phi F_u(A_e)$$

ϕ is a resistance reduction factor and is normally equal to 0.75 for design purposes. This resistance reduction factor accounts for the possibility of material imperfection, and the uncertainty level inherent in the failure mechanism. For the purposes of forensic engineering calculations, it is reasonable to assume a ϕ factor of 1.0 since the bolt manufacturers typically ensure their products exceed the minimum design strength. F_u is the ultimate fracture stress of the bolt, 60 ksi for A307 bolts. A_e is the net tensile area of one bolt, taking into account the reduction in tensile area due to the threads. Table 8-7 in AISC, 1995 lists a value of .226 in^2 for 5/8" diameter A307 bolts. The capacity of one 5/8" diameter A307 bolts is then equal to 60(.226) or 13.6 kips. The total resistive force of the eight anchor bolts is 108.5 kips. The total righting moment, M_r, is equal to the sum of the righting forces multiplied by their respective moment arms. In this case, M_r is equal to 108.5(15.5') + 67.27(7.75') or 2,203 ft*kips. Next, the overturning moment, M_o, due to the wind loading on the parachute tower was calculated using a modified form

of the basic wind load equation found in ASCE 7-95. The equation used in the spreadsheet is provided below and the detailed calculations can be found in Appendix A.

$$M_o = \Sigma[(q*G*C_p*A*e_z)/(I*K_z)]$$

G = Positive pressure gust effect factor, taken as 1.1
e_z = Moment arm of the wind force (ft)
C_p = External pressure coefficient
GC_{pi} = Combined gust factor and internal pressure coefficient
A = Projected area normal to wind force (ft^2)
I, K_z, & q_z were defined previously in Section 2.3

Using this approach, the overturning moment, M_o, was found to be 45.9q ft*kips, where q is the wind pressure on the structure. Equating the righting moment, M_r, and the overturning moment, M_o, and solving for q, the wind pressure was determined to be approximately 48.0 psf. The minimum wind velocity to cause failure is then calculated using the equation, $V = \sqrt{q/.00256}$. Using this equation the minimum failure wind velocity was found to be 136 mph.

It should be noted that an analysis of the failure of this structure was previously conducted by researchers at Texas Tech University using the ANSI A58.1-1982 standard (Mehta, 1976; McDonald et al., 1983). The wind speed calculations in this report were independently performed using the wind load provisions of ASCE 7-95. This independent analysis was performed to validate the earlier analysis. Even though some portions of the ASCE 7-95 vary substantially from the previous ANSI A58.1-1982 standard, the wind speeds estimated using both standards were very comparable. The earlier analysis calculated the wind speed to be 116 mph while an analysis using current codes shows the wind speed to be approximately 136 mph. The reason for the difference between the analyses is that the earlier analysis assumed that the wind pressure on the

windward wall was constant and did not vary with height, as did the current analysis.

Another contributing reason was that the external pressure coefficients changed for the

leeward wall and the roof from the ANSI A58.1-1982 standard to the ASCE 7-95

standard.

Points of Interest

Since the majority of the siding remained attached to the structure, the main

structural elements were subjected to the maximum wind loads possible. One could

speculate that if the siding had failed, the corresponding reduction in wind loading on the

main structure would have been sufficient to allow the main structure to survive.

4.3 Tornado at Altus, Oklahoma: Building 285

Location and Site Conditions

Building 285 is located on the east side of Altus AFB in Altus, Oklahoma. Altus is located in the southeast corner of Oklahoma, just north of the Texas border. The area around building 279 is generally unobstructed and classifies as open terrain, exposure C, as defined by ASCE 7-95.

Description of Structure

Building 285 is a large hangar that is approximately 500 feet wide, 600 feet long and 70 feet tall. The columns are standard wide flange shapes and the girders that span between the columns and run parallel to the short side of the building are custom fabricated trusses. The lateral load resisting system is made up of steel cross bracing. The exterior walls of the hangar are covered with asbestos cement (transite) siding of an unknown thickness and pattern. The roof is covered with sheets of 18 gage corrugated metal decking that is 30 inches wide and 8 feet long. The corrugations in the decking are 1-1/2 inches deep and the ribs are spaced 6 inches apart. The corrugated decking is covered by rigid insulation board. The insulation board is then covered by standard hot mopped, built up roofing. The front of the hangar is enclosed by a series of large door sections that are 65 feet tall and 20 feet wide. These door sections travel along a series of rails at the bottom and are restrained at the top by door guides.

Wind Speed Analysis

Building 285 was damaged by the Altus, Oklahoma tornado on May 11, 1982. A detailed description of this storm was provided earlier in Section 3.5. As shown by the

calculations in Section 4.2 of this chapter, the maximum wind speeds experienced near Building 285 were approximately 136 mph. This wind speed was estimated based on the previous analysis of the parachute tower failure.

Description of Damage

Overall, the hangar performed well when subjected to these severe winds. The exterior corrugated asbestos siding performed well and experienced only localized failure. There were no failures noted in the heavy "C" channel wall girts or the roof trusses supporting the corrugated siding and the roof decking, respectively. No failures were noted on the main structural elements. The only damage to this building was the removal of a portion of the roofing material and the roof decking, structural damage to two rail mounted hangar door sections, and the removal of exterior corrugated siding along the door pockets. The damage to the hangar is shown in Figures 4.12 through 4.17.

Figure 4.12 Aerial View of Damage to Building 285
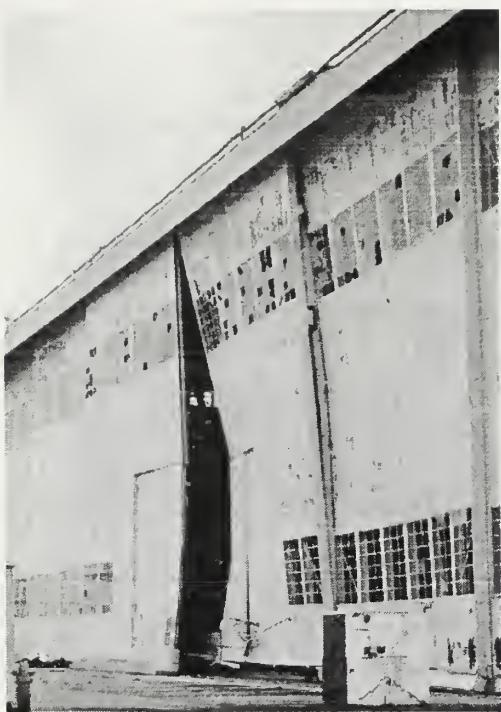
Figure 4.13   Elevation of the North
              Side of Bldg 285
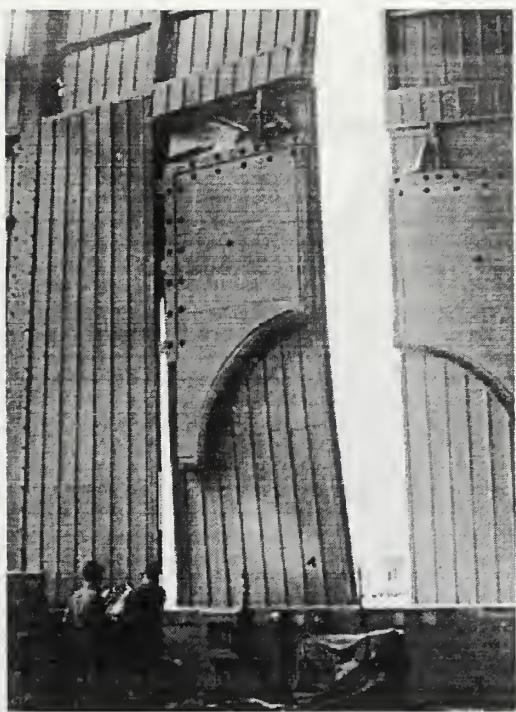

Figure 4.14 Interior Elevation of Damaged
             Hangar Door
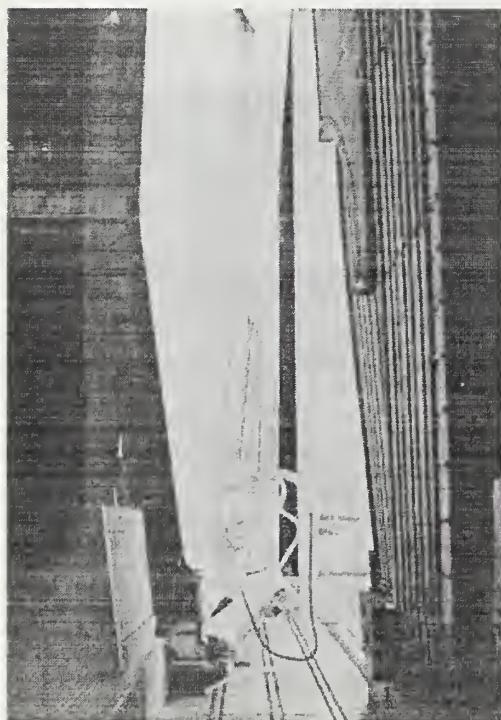
Figure 4.15   Section View of Damaged
              Hangar Door
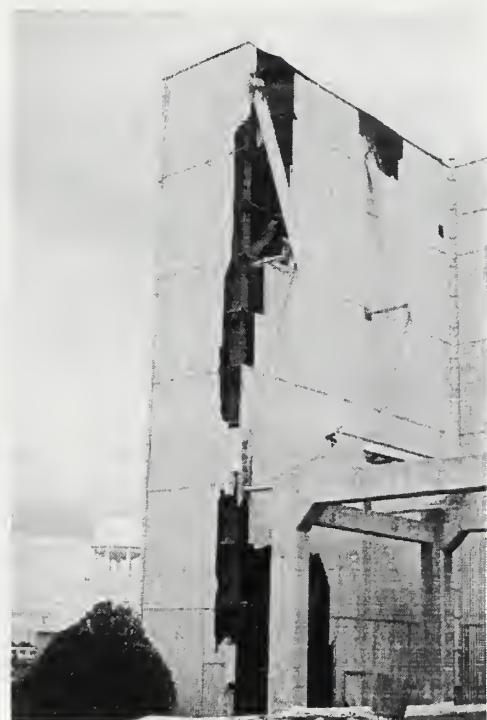
Figure 4.16 Damage to NW Hangar
             Door Pocket
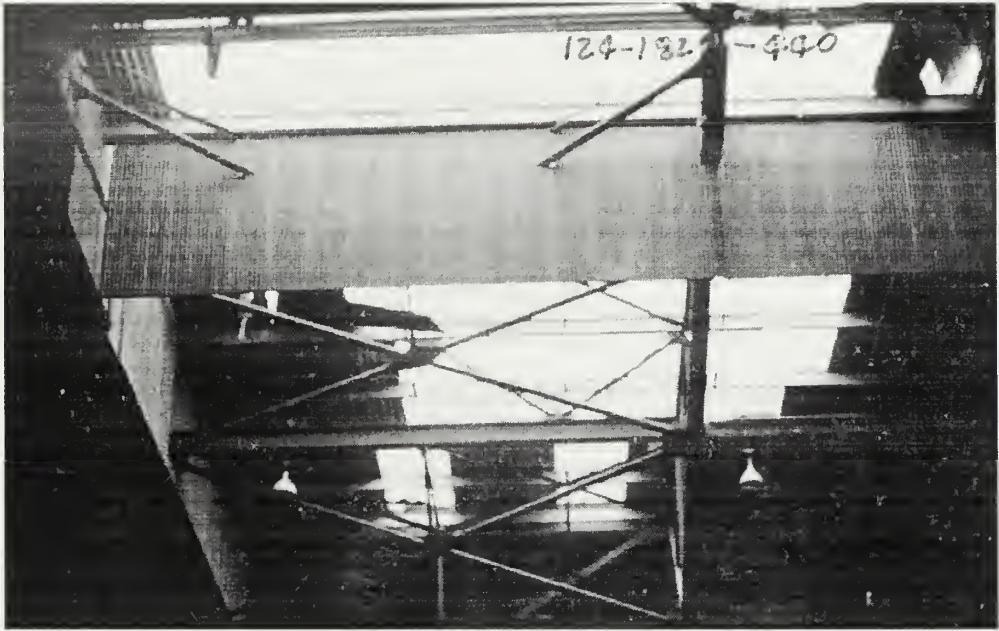
Figure 4.17 Interior of Building 285, NW Corner of Roof

Figure 4.18 Damaged Corrugated Roof Panel, Building 285

<u>Analysis of Damage</u>

As previously mentioned, the elements of the structure that were damaged include two sections of the hangar doors, the corrugated siding, the roof covering, and the roof decking. Since this structure is located over 500 miles from the nearest coastline, the maximum design wind speed used by the designers was probably less than 100 mph. Since the wind speeds experienced by the structure were approximately 30 percent faster than the design wind speed, the resulting loads were over 50 percent larger than the design loads. Under these extreme wind loads, the small amount of damage as seen in the previous figures is expected. However, an analysis of the damage is still useful to determine the weak points in the structure and identify areas where improvements can easily be made.

The partial failure of two sections of the hangar door, as seen in Figures 4.13, 4.14, and 4.15 was caused by wind acting normal to the door surface and weakness in the free edges of the door sections. Because of the secondary openings in the door sections, they did not have a continuous member along their free edge. This lack of a continuous member weakened the structural framing and the lighter secondary framing was unable to transfer the loads into the upper header and the lower rail seen in Figure 4.15. This failure was most likely <u>not</u> due to either a design or a construction deficiency but was simply an area of the structure that had little redundancy.

The majority of the damage to the roof covering seen in Figure 4.12 is along the edges of the roof line. This damage is consistent with the higher suction pressures that are typically experienced at the leading edges of a structure with a flat roof. One other factor that may have precipitated the damage to the roof membrane is the partial failure of

the metal edge flashing seen in Figure 4.13. When this edge flashing failed, it allowed wind to propagate under the roof membrane thus causing failure of the roof membrane located just under the flashing. The failure of this edge flashing can be directly attributed to the lack of a retaining cleat on the free edge of the flashing as specified by the SMACNA Architectural Sheet Metal Manual, 1993.

The localized failure of the corrugated metal decking can be seen in Figure 4.17. It is important to note that the decking only failed in one, highly localized area, where the structure would have experienced the largest peak roof suction pressures. As can be seen in Figure 4.18, the corrugated decking was tack welded to the structural framing at each of the ribs. Although the size and quality of the tack welds is still questionable, it is reasonable to assume that construction problems were not the major factor in the decking failure. The only other factor that could have contributed to the failure of the corrugated roof decking is the prior partial failure of the hangar doors. When the hangar door sections deflected, this may have allowed the internal pressure in the hangar to increase. This increased positive internal pressure would then combine with the roof suction pressure and contribute to the failure of the decking at the locations of the highest external suction pressure.

The localized damage to the corrugated siding can be seen in the aerial photograph of the hangar, Figure 4.12 and on an exterior elevation of the door pocket, Figure 4.16. The damage seen in Figure 4.16 is primarily due to high localized suction pressure caused by wind acting normal to the front face of the hangar. The localized failure of the siding was caused by the high suction pressures generated by the normal wind and by the irregular shape of the structure. Another factor that could have

contributed to the failure of the siding was the prior partial failure of the two hangar door sections. When the hangar door sections deflected, this may have allowed the internal pressure inside the hangar and the door pocket to increase. This increased positive internal pressure could combine with the high leeward suction pressure and contribute to the siding failure.

Points of Interest

One significant point to note about the damage to this structure is that the main structural system sustained virtually no damage even though the applied wind loads may have been over 50 percent larger than the design loads. Another point to note is the good performance of the girts and corrugated siding. In fact, the siding experienced only localized damage at each of the south hangar door pockets. The performance of the girts and siding can be mainly attributed to the narrow girt spacing, approximately four feet, and the excellent performance of the main structural system. Although there was no significant damage to the main structural elements, there are several essential points to note about the damage to the hangar doors, siding, and roofing.

The only failure of the roofing and siding were in areas of flow separation, thus areas of very high suction pressure. These areas are the same areas where the wind tunnel testing described in Section 2.2 underestimated the peak suction pressures.

4.4 Hurricane Gilbert: Large Warehouse Building

Location and Site Conditions

The structure is located on Kelly Air Force Base in San Antonio, Texas. San Antonio is located approximately 150 miles north of the Gulf of Mexico as shown in Figure 3.2. Since this building is located in an area of the base adjacent to one of the large runways, the terrain can be classified as open and unobstructed, exposure C, as defined by ASCE 7-95.

Description of Structure

The structure is a large flat roofed supply warehouse with exterior concrete masonry unit (CMU) walls. The main structural components include interior wide flange columns, custom designed open web steel joists running the length of the building, and standard open web steel joists spanning the width of the building. The lateral wind loads are transferred to the foundations via CMU shear walls.

Analysis of Wind Speed

The large supply warehouse was damaged by a tornado that was spawned by Hurricane Gilbert as it passed some 120 miles south of San Antonio as shown previously in Figure 3.2. Since this structure is located far inland and away from the path of Hurricane Gilbert, it felt virtually no direct effects of the hurricane winds.

There is very little data available on the wind speeds generated by the tornado that caused the damage to this structure. Also since no "simple" structures were damaged in the immediate area, back calculation of the wind speed is not possible. However, the

tornado was rated a weak F3 based on the damage done to several buildings in the area. The F3 damage indicates wind speeds between 150 and 170 mph.

Description of Damage

The main structural system performed well and sustained very little damage as did the large overhead doors, shown in Figure 4.19. The only damage to the main structural system was a horizontal crack in the CMU shear wall. The other element damaged was the corrugated steel roof decking. Approximately 80% of the corrugated steel roof deck was torn from the building. The damage mentioned can be seen in 4.20 and 4.21.

Figure 4.19 Undamaged Overhead Door
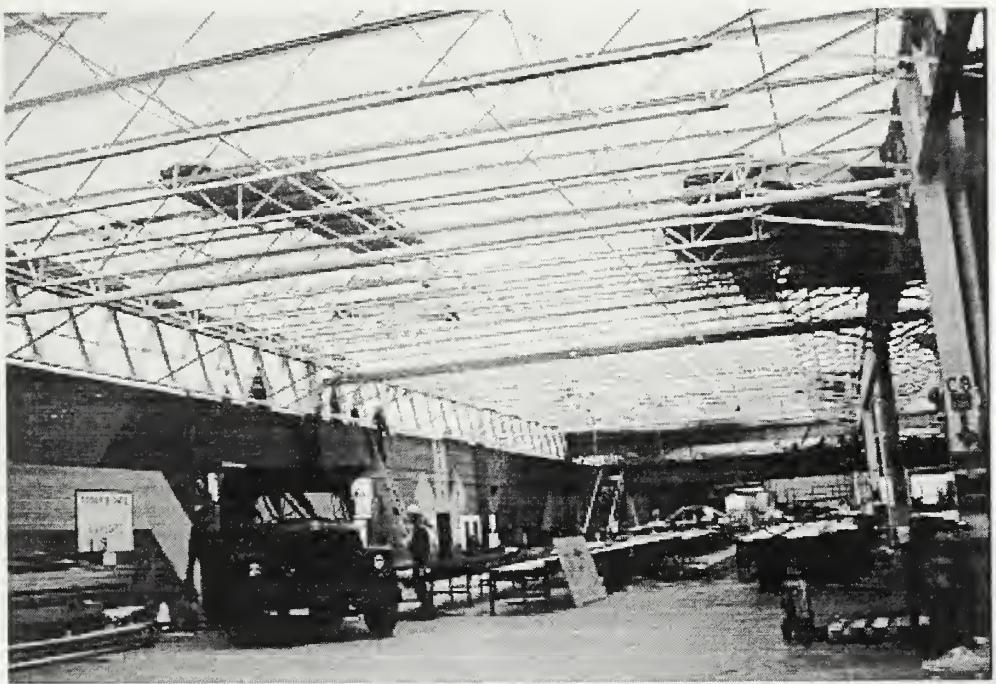
Figure 4.20 Interior of Supply Warehouse
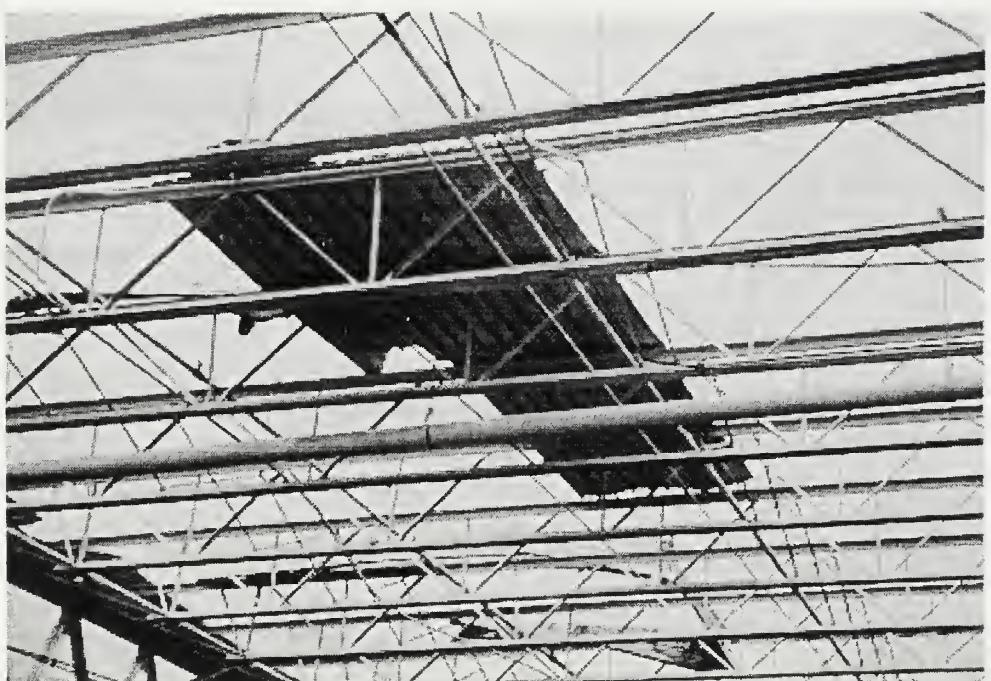
Figure 4.21 Damaged Corrugated Roof Panel

Analysis of Damage

Since the overhead doors performed well and no other openings in this structure failed, an increase in the building internal pressure could not have been a contributing factor in the failure of the roof decking. The decking either failed because of inadequate spot welding or because the external pressure on the roofing exceeded the strength of the roofing material. Since the roof damage was so extensive and since there was little roof damage to similar structures in the area, the failure was most likely caused by a inadequate attachment of the roof panels. Although not definitive, the inconsistency in the spot welding can be deduced from careful inspection of Figure 4.21. As shown in Figure 4.21, only the spot welds on the outside ribs held. The welds on the interior ribs either failed prematurely or were never completed.

Points of Interest

Again, one point to note is that the main structural system of the building performed very well. Although the wind loads were probably at or above design levels, none of the main structural elements sustained any damage. The other item to note is that the failure of the corrugated roof panels was not precipitated by the failure of any other exterior cladding components. The final item worth noting is that none of the roof panels along the edges of the roof wall junction remained. This is significant because the roof wall junctions are the areas where tests have indicated the highest external suction pressures.

4.5 Hurricane Hugo: Large Aircraft Hangar

Location and Site Conditions

The subject structure is located on Charleston Air Force Base in Charleston, South Carolina. Charleston AFB is located less than a mile from the Atlantic coast as seen in Figure 3.3. This building is located adjacent to one of the large runways, thus the terrain can be classified as open and unobstructed, exposure C, as defined by ASCE 7-95.

Description of Structure

The large hangar is very similar to the hangar that was previously examined in Section 4.3. The structure is approximately 500 feet wide, 600 feet long and 60 feet tall. The designers used standard wide flange shapes for the columns. The girders that span between the columns and run parallel to the short side of the building are custom fabricated trusses. The lateral load resisting system is made up of steel cross bracing. The exterior walls of the hangar are covered with corrugated metal siding of an unknown thickness and pattern. The virtually flat roof is also covered with sheets of 22 gage corrugated metal decking of an unknown pattern. The corrugated decking is covered by rigid insulation board and the insulation board is then covered by standard hot mopped, built-up roofing. The front of the hangar is enclosed by a series of large door sections. These door sections travel along a series of rails at the bottom and are restrained at the top by door guides.

Wind Speed Analysis

The subject structure was damaged by Hurricane Hugo as is passed near Charleston, South Carolina on September 22, 1989. A detailed description of this storm

was provided earlier in Section 3.3. Wind data on this storm was available from a variety of sources, but the closest reliable anemometer data was obtained from Charleston WBAS. This weather station recorded a peak gust of 85 kts at an elevation of 20 feet in exposure C (McDonald et al., 1990). The term peak gust from the reporting weather station is interpreted as a one to two second average. Since the defining parameters of the reported wind speed differ from the standard values, they must be converted. After the appropriate conversions have been applied the equivalent three second gust velocity at 33 feet above ground in exposure C is calculated to be 108 mph. Since this peak wind speed is well below the design wind speed specified by either ASCE 7-88 or ASCE 7-95, the structure should have sustained very little damage, if any.

Description of Damage

The only visible damage to this hangar is damage to the roof covering and decking. All of the structural members performed as designed, as did the corrugated metal siding. All of the windows in the structure remained intact, as did the hangar doors. These observations of the extent of the damage generally agree with the assessment by McDonald and Smith, 1990. The extent of the damage can be seen in Figures 4.22 and 4.23.

Figure 4.22 Exterior Elevation of Large Hangar

Figure 4.23 Interior Elevation of Large Hangar

Analysis of Damage

It appears that the roof decking was lifted off the joists by suction pressure that formed due to wind acting normal to the hangar doors. Since none of the windows on the exterior of the structure were damaged and the hangar doors were also undamaged, it is unlikely that a large increase in the buildings internal pressure could have contributed to the damage of the panels. If the provisions of ASCE 7-95 are applied to the wind recorded velocity of 108 mph and an internal pressure coefficient of +/- .18 is used, the decking had to resist a total suction pressure of 33 psf. The equations used to calculate this pressure are $p = qGC_p - q(GC_{pi})$ and $q = 0.00256*K_z*I*V^2$. The details of the calculations made to obtain this pressure are as follows $q = (.00256*1.17*1*108^2) = 34.9$ psf and $p = (34.9*.85*-.9) - (34.9*.18) = 33$ psf. Since this pressure is well below the required building code value, either the contractor did not properly fasten the decking with spot welds or ASCE 7-95 underestimates the peak suction pressures at areas of flow separation.

Points of Interest

Once again, one point to note is that the main structural system of the building performed very well. Although the wind loads were near design levels, none of the main structural elements sustained any damage. The other item to note is that the roof decking failed when subjected to wind velocities and pressures below design values. The area of the failure was also limited to the windward wall/roof junction, similar to the damage observed on building 285 on Altus, AFB. The final item of interest is that the damage observed on the two hangars is very similar despite the fact that one was damaged by a hurricane and the other was damaged by a tornado.

4.6 Hurricane Andrew: Aircraft Hangars

Location and Site Conditions

The subject structures are located at the Miami International airport in Miami,
Florida. The approximate location of the structure is indicated Figure 3.4 along with the
proximity of the storm path to the structures. The area is flat with few obstructions and
classifies as exposure C as defined by ASCE 7-95.

Description of Structures

The Beechcraft hangar shown in Figures 4.23, 4.24, and 4.25 is approximately
200 feet long, 60 feet wide, and 40 feet tall. The structure has a gable roof with a very
slight pitch (approximately 1/4" per foot). The exterior walls are covered with corrugated
metal siding and the roof is covered with corrugated metal decking. The main structural
system is made up of wide flange steel columns, large custom girders, and z shape roof
purlins. The lateral loads are transferred to the foundation via steel cross bracing running
between the columns. All of the main structural elements can be seen in Figure 4.25.
The other two hangars that are shown in Figure 4.26 are very similar in size and
construction to the Beechcraft hangar.

Analysis of Wind Speed

The three structures shown in Figures 4.23 through 4.26 were all damaged by
Hurricane Andrew in August of 1992. Since these structures are located at an airport,
reliable anemometer data was readily available. Anemometers at the site recorded a
velocity of 115 mph for the maximum three second gust at 33 feet above ground level
(Marshall, 1992).

Description of Damage

The main component that was damaged on all three hangars was the roof decking. The corrugated siding on the front of the Beechcraft hangar also received minor damage at the door pocket, see Figure 4.25.

Figure 4.24 Elevation of Beechcraft Hangar

Figure 4.25 Elevation of Beechcraft Hangar

Figure 4.26 Interior Elevation of Beechcraft Hangar

Figure 4.27 Aerial View of Two Damaged Hangars

Analysis of Damage

The pattern of failure of the roof decking is very similar to that seen in the previous structures. The roof decking performed well over the majority of the roof and failed only within four to six feet of the edge of the windward wall. Since the roof decking used on these hangars was attached with screws at an interval determined by the manufacturer's catalog data, it is unlikely that construction error is the cause of the failure. In addition, since the wind velocities were less than 120 mph, the roof decking should not have sustained any damage.

Points of Interest

One main point to notice is that the primary structure performed very well and sustained virtually no damage. Another important point is that when the roof decking

was torn from the purlins, the purlins were left undamaged. This indicates that either there were an insufficient number of fasteners or the fasteners did not have sufficient contact surface area with the decking to prevent localized failure of the decking material around the head of the fasteners.

CHAPTER 5

CONCLUSIONS & RECOMMENDATIONS

The case studies provided in this report are examples of the types of damage that was observed on low rise open span steel structures. Similar damage to numerous other structures is documented in the Texas Tech Wind Library, but due to the limited space available for this report, the number of case studies was limited to those given.

Although many examples of damage were observed in the preparation of this report, and the patterns of failure were all found to be very similar, care must be taken in drawing conclusions from such rough analysis. Likewise, the conclusions that are reached should be kept in the context of the report and the limitations of the available wind velocity data and other parameters should be carefully considered. However, as limited as the data is, it does provide valuable qualitative information about the performance of low-rise heavy steel structures when subjected to design level wind velocities.

5.1 Conclusions

The main structural systems of the buildings studied all performed very well. In fact, after reviewing over 1000 damage photographs from seven different storm events, no instance of main structural failure was noted for a low rise, heavy steel structure. The excellent performance of the main structural systems is most likely the result of a combination of one or more of the following factors:

1) Good prediction of the total wind loads by the wind standards.

2) The large degree of structural redundancy in heavy steel structures.

3) Good construction practices and qualified workers on these larger, custom designed projects.

4) Code requirements for the connections to be stronger than the structural members being joined together.

In contrast to the excellent performance of the main structural systems, the overhead doors performed poorly. In numerous instances, the overhead doors were the first components to fail. Their initial failure then precipitated further damage to the structure such as damage to the roof decking and exterior wall cladding. Although a detailed analysis of the failure of the overhead doors was not conducted, several other researchers have noted similar damage and have found that typically excessive deflection in the door curtains allows the rollers to rotate out of the guide rails, thus causing the failure of the doors (FEMA, 1992).

Another component that performed very poorly were the roof panels. In almost every instance of damage to a heavy steel structures, the roof decking failed at the junction of the windward wall and the roof. This failure was noted regardless of the fastening system, whether spot welding or screws. This consistent failure could be the result of construction errors, design errors or an underestimation of the peak loads by the wind standards. Construction error is a possibility, but it is highly improbable that the errors would be made in the same areas on a variety of structures built by different contractors. Design errors can explain some of the failures since current practice does not require additional fasteners in areas of higher suction pressure. Another viable explanation for the consistent damage is that the design wind standards underestimation of the peak suction pressures in areas of flow separation.

5.2 Recommendations

The recommendations made in this report deal primarily with the construction and design of overhead doors, roof decking, and wall siding. Much more design attention needs to be placed on the specification of certified overhead doors if the buildings are constructed in high wind areas or house high value materials. There are currently many manufacturers that offer commercially available doors that have the structural capacity to resist design wind velocities. These manufacturers can provide test results from Underwriter's Laboratory (UL) or other independent testing agencies to prove their viability.   Since quality doors are available, it is the responsibility of the design engineer to specify the proper door and educate his client as to its importance. Although providing quality overhead doors will not ensure that the structure is not damaged, without it, extensive damage is a foregone conclusion.

The poor performance of the roof decking and wall siding in areas of peak suction pressure needs to be addressed in a different manner. In the short run, designers should increase the number of fasteners used on roof and wall siding in areas where high peak suction pressures can occur, namely at roof/wall junctions and at sharp changes in building geometry. In the long run, more research needs to be done to ensure that the peak cladding wind loads specified in the design standards are adequate in areas of flow separation.

REFERENCES

AISC, (1995), Manual of Steel Construction - Load & Resistance Factor Design, Volume 1, Second Edition, American Institute of Steel Construction, Chicago, Illinois

ASCE, (1995), *Minimum Design Loads for Buildings and Other Structures*, ASCE 7-95, American Society of Civil Engineers (ASCE), New York, New York.

FEMA, (1992), "Building Performance in Hurricane Andrew in Florida", Federal Emergency Management Agency/Federal Insurance Administration, Miami, Florida.

Greenberg, Keith, (1994), *When Disaster Strikes - Hurricanes and Tornadoes*, Twenty-First Century Books, New York, New York.

Marshall, T. P., (1992), "Hurricane Andrew Storm Damage Survey", Haag Engineering Co., Dallas, Texas.

Marshall, T. P., McDonald, J. R., Mehta, K.C., (1983), "Utilization of Load and Resistance Statistics in a Wind Speed Assessment", Institute for Disaster Research, Texas Tech University, Lubbock, Texas.

McDonald, J. R., Marshall, T. P., (1983), "Damage Survey of the Tornadoes Near Altus, Oklahoma on May 11, 1982", Institute for Desaster Research, Texas Tech University, Lubbock, Texas.

McDonald, J. R., Mehta, K. C., (1987), "Wind Characteristics of Tornadoes", Proceedings from the WERC/NSF Wind Engineering Symposium (November 2-4, 1987 Kansas City, Missouri), Engineering Conference, Columbia, Missouri.

McDonald, J. R., Smith, T. L., (1990), "Performance of Roofing Systems in Hurricane Hugo", Institute for Disaster Research, Texas Tech University, Lubbock, Texas.

Mehta, K. C., (1976), "Windspeed Estimates in Tornadoes: Engineering Analysis", *Proceedings of the Symposium on Tornadoes: Assessment of Knowledge and Implications for Man*, Texas Tech University, Lubbock, Texas.

Mehta, K. C., Marshall, R. D., and Perry, D. C., (1991), *Guide to the Use of the Wind Load Provisions of ASCE 7-88*, American Society of Civil Engineers, New York, New York.

Mehta, K. C., Minor, J. E., McDonald, J. R., and Reinhold, T. A., (1981), "Valuable information from Wind-Caused Damage in Hurricane Frederic," *Proceedings of the Fourth U. S. National Conference on Wind Engineering Research*, University of Washington, Seattle, Washington.

Palm Beach Post (1996), "History of Hurricanes", Http://www.pbpost.com/storm96/guide/history.htm, Palm Beach Post, Palm Beach, Florida.

Reinhold, T. A. (1979), "Surface Winds from Hurricane Frederic (September 12 & 13, 1979) an Engineering Viewpoint," National Bureau of Standards, Washington, D. C.

Simiu, E., Scanlan, R. H., (1996), *Wind Effects on Structures*, Third Edition, John Wiley & Sons, Incorporated, New York, New York.

SMACNA, (1993), *Architectural Sheet Metal Manual*, Sheet Metal and Air Conditioning Contractors National Association, Chantilly, Virginia.

Stathopoulos, T., (1983), "Scale Effects in Wind Tunnel Testing of Low Rise Buildings," *Journal of Wind Engineering and Industrial Aerodynamics*, Vol. 13, pp. 313-326, Elsevier Science Publishers, B.V., Amsterdam.

Property Claim Service, (1996), *Wind Engineering Research Center Newsletter*, Texas Tech University, Lubbock, Texas.

APPENDIX A

TABLE OF CONTENTS

APPENDIX A

Wind Conversion Equations

Logarithmic Law

Basic Equation

$$U(z) = 2.5 * U^* \ln(z/z_0)$$

$U(z)$: Mean wind velocity at height z U^*: Friction velocity for a given terrain
   z: Height above ground z_0: Roughness length for a given terrain

Modified Form for Converting Heights

$$\frac{U(z_1)}{U(z_2)} = \frac{\ln(z_1/z_0)}{\ln(z_2/z_0)}$$

$U(z_1)$: Mean wind velocity at height z_1 $U(z_2)$: Mean wind velocity at height z_2
   $z_{1\&2}$: Height above ground z_0: Roughness length for a given terrain

Modified Form for Converting Averaging Times

$$R_t = \frac{U_t(z)}{U_{3600}(z)} = 1 + \frac{\sqrt{\beta} * c(t)}{2.5 * \ln(z/z_0)} \qquad U_x = U_{3600} * R_x$$

   $U_t(z)$: Mean wind velocity at height z averaged over time t seconds
$U_{3600}(z)$: Mean wind velocity at height z averaged over time of 3600 seconds
      β: Variable to account for the change in the fluctuations in the longitudinal
          turbulence for different roughness lengths
     $c(t)$: Variable to account for the difference between the sample averaging time and
          the averaging time of 3600 seconds

CONVERSION OF FUJITA SCALE FASTEST 1/4 MILE WIND
TO A FASTEST 3 SECOND WIND

1/4 Mile Wind Speed	t_{avg}	β	$c(t_{avg})$	z	z_o	R_1	U_{3600}	$c(t_3)$	R_2	U_3
40	22.500	6	1.9325	33	0.2297	1.3812	28.961	2.849	1.5619	45.24
72	12.500	6	2.24	33	0.2297	1.4418	49.937	2.849	1.5619	78.00
73	12.329	6	2.2455	33	0.2297	1.4429	50.592	2.849	1.5619	79.02
112	8.036	6	2.468	33	0.2297	1.4868	75.330	2.849	1.5619	117.66
113	7.965	6	2.4738	33	0.2297	1.4879	75.944	2.849	1.5619	118.62
157	5.732	6	2.6424	33	0.2297	1.5212	103.208	2.849	1.5619	161.21
158	5.696	6	2.6452	33	0.2297	1.5217	103.829	2.849	1.5619	162.17
206	4.369	6	2.7455	33	0.2297	1.5415	133.634	2.849	1.5619	208.73
207	4.348	6	2.7471	33	0.2297	1.5418	134.256	2.849	1.5619	209.70
260	3.462	6	2.8140	33	0.2297	1.5550	167.198	2.849	1.5619	261.15
261	3.448	6	2.8150	33	0.2297	1.5552	167.820	2.849	1.5619	262.12
318	2.830	6	2.8617	33	0.2297	1.5645	203.266	2.849	1.5619	317.49

Weight Calculations for Parachute Drying Tower
Damaged in Altus, Oklahoma Tornado

Component	Member Size	Wt/ft^2	Length (ft)	Width (ft)	Area (ft^2)	No. of Areas	Weight (lbs)
				WALLS			
Corrugated Asbestos Siding		3.5	49.71	28.5	1,417	2	9,917
		3.5	49.71	15.5	771	2	5,394
Framing - Vertical	2x4 @ 24" o.c.	0.7	61.375	28.5	1,749	2	2,449
Framing - Horizontal	1x3 @ 16" o.c.	0.4	61.375	15.5	951	2	761
Wall Insulation	Batt Ins.	0.7	61.375	26.5	1,626	2	2,277
		0.7	61.375	13.5	829	2	1,160
1/4" Asbestos Bd.		2	61.375	26.5	1,626	2	6,506
		2	61.375	13.5	829	2	3,314
				ROOF			
Built Up Roofing		6	15.5	28.5	442	1	2,651
Metal Roof Deck		2	15.5	28.5	442	1	884
Roof Insulation	Rigid Board	1	15.5	28.5	442	1	442
Framing	2x4 @ 24" o.c.	0.7	15.5	28.5	442	1	309
Framing	1x3 @ 16" o.c.	0.4	15.5	28.5	442	1	177
Fixtures & Ceiling		3	13.5	26.5	358	1	1,073
Ceiling Insulation	4" Batt	1	13.5	26.5	358	1	358
Steel Grating		5.7	13.5	26.5	358	1	2,039
						Total Coverings =	39,709

Description	Member Size	Wt/ft	Length (ft)	No. of Members	Weight (lbs)
		STRUCTURAL STEEL			
Columns	W6x15.5	15.5	62.33	4	3,864
Cross Brace	L3x2-1/2x1/4	4.5	13.46	6	363
Cross Brace	L3x2-1/2x1/4	4.5	11.88	2	107
Cross Brace	L3x2-1/2x1/4	4.5	15.13	2	136
Cross Brace	L4x3x1/4	5.8	18	6	626
Cross Brace	L4x3x1/4	5.8	16.85	2	195
Cross Brace	L4x3x1/4	5.8	19.29	2	224
Wall Beam	W10x21	21	28.5	8	4,788
Wall Beam	8B13	13	15.5	8	1,612
Wall Girt	C8x11.5	11.5	15.5	8	1,426
Wall Girt	C8x11.5	11.5	28.5	8	2,622
Per. Floor Beam	W16x36	36	15.5	2	1,116
Per. Floor Beam	W16x36	36	28.5	2	2,052
Floor Girder	W12x27	27	28.5	3	2,309
Floor Beam	I3x5.7	5.7	15.5	9	795
Roof Beam	W10x21	21	15.5	2	651
Roof Beam	W12x27	27	28.5	2	1,539
Roof Joist	8B4.5	4.5	15.5	9	628
				Subtotal =	25,054
Bolts and Misc.	10% of steel subtotal				2,505
				Total Steel =	27,559

Total Bldg Wt = 67,269 lbs

Calculations to Determine Gust Effect Factor

For Parachute Drying Tower

For exposure C $\qquad \varepsilon = 1/5.0 \qquad c = .20 \qquad \ell = 500'$
$\qquad\qquad\qquad\qquad\qquad b = 15.5' \qquad h = 62.3' \qquad z = 62.3'$

$$G = 0.9\left[\frac{\left(1 + 7I_z Q\right)}{1 + 7I_z}\right] \qquad \text{Equation (C6-5)}$$

$$I_z = c(33/z)^{1/6} \qquad\qquad \text{Equation (C6-6)}$$

$$Q^2 = \frac{1}{1 + .63\left(\dfrac{b+h}{L_z}\right)^{.63}} \qquad \text{Equation (C6-7)}$$

$$L_z = \ell(z/33)^{\varepsilon} \qquad\qquad \text{Equation (C6-8)}$$

$$I_z = .20(33/62.3)^{1/6} \qquad\qquad I_z = .18$$

$$L_z = 500*(62.3/33)^{1/5.0} \qquad\qquad L_z = 567.8$$

$$Q^2 = \frac{1}{1 + .63\left(\dfrac{15.5 + 62.3}{567.8}\right)^{.63}} \qquad Q^2 = .92$$

$$G = 0.9\left[\frac{\left(1 + 7*.18*.92\right)}{1 + 7*.18}\right] \qquad G = .86$$

Wind Load Calculations for Parachute Tower
Damaged in Altus, Oklahoma Tornado

Beginning Height (ft)	Ending Height (ft)	1	Kz	G	Cp	Area (ft²)	e (ft)	Moment (ft*lbs)
Windward Moment								
13	15	1	0.85	0.86	0.8	57	14	646
15	20	1	0.9	0.86	0.8	142.5	17.5	1,906
20	25	1	0.94	0.86	0.8	142.5	22.5	2,347
25	30	1	0.98	0.86	0.8	142.5	27.5	2,751
30	40	1	1.04	0.86	0.8	285	35	6,599
40	50	1	1.09	0.86	0.8	285	45	8,095
50	62	1	1.13	0.86	0.8	342	56	11,661
Leeward Moment								
13	62	1	1.13	0.86	0.7	441.75	37.5	8,825
Roof Moment								
62	62	1	1.13	0.86	0.3	442	7.75	782
Internal Pressure Moment								
13	62	1	1.13	1	0.18	1396.5	7.75	1,724
62	62	1	1.13	1	0.18	442	7.75	546
							Total =	45,882